Heliyon 9 (2023) e16613

Contents lists available at ScienceDirect

Heliyon

journal homepage: www.cell.com/heliyon

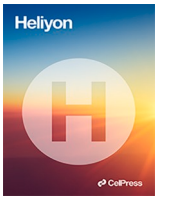

Research article

Protective effects of Liupao tea against high-fat diet/cold exposure-induced irritable bowel syndrome in rats

Danshui Zhou [a,1], Xiaotong Liu [a,1], Lunli Lan [b], Wenxin Yu [a], Ruijin Qiu [c], Jianhua Wu [c], Cuiqin Teng [c], Liyun Huang [c], Cuiping Yu [c], Yu Zeng [a,*]

[a] School of Traditional Materia Medica, Guangdong Pharmaceutical University, Guangzhou, Guangdong, China
[b] College of Pharmacy, Guilin Medical University, Guilin, Guangxi, China
[c] Wuzhou Institute of Agricultural Sciences, Wuzhou, Guangxi, China

ARTICLE INFO

Keywords:
Liupao tea
Irritable bowel syndrome
High-fat diet/cold exposure
AQP3
Gut microbiota

ABSTRACT

Liupao tea as a type of dark tea can relieve irritable bowel syndrome by regulating gut microbiota, but the mechanism has not been fully explained. An ultra-high performance liquid chromatography along with quadrupole time of flight tandem mass spectrometry was used to analyze the phytochemicals in Liupao tea. Then, we explored the effects of Liupao tea against IBS. From the results of chemical analysis, we identified catechins, polyphenols, amino acids, caffeine, polysaccharides and other components in Liupao tea. The open-field test, gastrointestinal function-related indexes, histochemical assays, measurements of cytokine and aquaporin 3 (AQP3), and determination of serum metabolites were utilized to monitor the physiological consequences of Liupao tea administration in rats with irritable bowel syndrome. The results showed that Liupao tea had a significant protective effect on irritable bowel syndrome. Liupao tea increased locomotive velocity while reducing interleukin-6, interleukin-1β, and tumor necrosis factor-α levels, as well as gastrointestinal injury. Moreover, Liupao tea increased the AQP3 levels of renal tissues but reduced the AQP3 levels of gastrointestinal tissues. Liupao tea reduced the *Firmicutes/Bacteroides* ratio and significantly reconstructed the microbial pattern. Liupao tea relieved irritable bowel syndrome by repairing gastrointestinal dysfunction, regulating the secretion of pro-inflammatory cytokines, modulating water metabolism, and restoring microbial homeostasis.

1. Introduction

Irritable bowel syndrome (IBS), one of the most common functional gastrointestinal disorders, has an incidence of approximately 10–22% in the general population [1]. Patients with IBS usually suffer from dyspepsia, chronic idiopathic constipation, diarrhea, abdominal pain [2], all of which greatly affect the individual's quality of life. It is reported that patients experience abdominal pain alongside alterations in the stool frequency and stool form at least once a week. Bloating is another common symptom [3]. IBS substantially contributes to direct or indirect costs due to unnecessary or too-frequent testing, which represents a huge burden on health care systems worldwide.

Studies have identified cold stress as a source of acute physical stress in animal models and indicated that abnormalities in cold

* Corresponding author.
E-mail address: zengyugdcpu@163.com (Y. Zeng).
[1] These authors contributed equally to this work.

https://doi.org/10.1016/j.heliyon.2023.e16613
Received 8 November 2022; Received in revised form 17 May 2023; Accepted 22 May 2023
Available online 27 May 2023
2405-8440/© 2023 The Authors. Published by Elsevier Ltd. This is an open access article under the CC BY-NC-ND license (http://creativecommons.org/licenses/by-nc-nd/4.0/).

stress-induced animal models resemble those in human IBS models [4]. Besides external stress, the most important factor that causes symptoms in patients with IBS is their feeding habits [5]. The consumption of saturated and *trans*-fats in lard might increase the secretion of pro-inflammatory cytokines in patients on a high-fat diet [6]. Diets based on lard oil have been previously studied [7,8]. In other words, internal exposure to foods and beverages induces major gastrointestinal symptoms and the external exposure to cold environment aggravates body abnormalities. In this study, we developed an animal model that mice were subjected to unhealthy diet and cold environment.

In the human body, aquaporins (AQPs) were considered important tools in the water transport system. AQPs are transmembrane channels facilitating water transit across biological membranes. Nowadays, the aquaporin family has been known to consist of 13 members (AQP0–12). AQP3, also known as aquaglyceroporin, belongs to the aquaporin family [9]. It is known that AQP3 is essential in intestinal function (it acts as a natural barrier) and urine concentration. AQP3 is abundant in the colonic epithelium and basolateral plasma membranes of the collecting duct's principal cells [10]. As several studies have confirmed that IBS changes water transport through AQP3 in the gastrointestinal tract and kidney, we are eager to figure out the exact mechanism of water transit through AQP3 when it comes to rats with IBS. We also notice that the imbalanced release of pro-inflammatory cytokines has been reported in IBS. Levels of interleukin-6 (IL-6), interleukin-1β (IL-1β), and tumor necrosis factor-α (TNF-α) are positively correlated with IBS symptoms in blood cytokine profiles of mice with IBS [11]. Since the regulation of these cytokines plays an important role in immune response and the activation of the NF-κB pathway [12], the expression levels of cytokines are also indispensable factors in this work. The last decades have witnessed an intensive investigation of the gut microbiota. Compared with healthy individuals, most patients with IBS have altered microbial profiles of diversity, stability, and metabolic activity [13]; thus, we need to pay attention to the altered pattern of the vast microbial community in rats with IBS.

Although caring for IBS patients in pain is a challenging issue for physicians without organic findings to explain the obstructive-like appearance during surgery, scientists have pointed out that these patients' imbalanced flora could be altered by probiotics, with a reduction in the intensity of abdominal pain and bloating [10]. The benefits of probiotics against IBS have been demonstrated by some experts [11], while others highlight the role of herbal traditional Chinese medicine for its efficiency via evidence-based trials [2], which implies that traditional Chinese medicine principles should not be ignored in this work when tackling IBS-related issues. On the one hand, a double-blinded randomized controlled trial proved that the Chinese herbal formula, Huoxiang Zhengqi, can relieve diarrhea-predominant IBS symptoms [14]. In clinical practice, the Huoxiang Zhengqi liquid is one of the Chinese patent medicines that are most frequently used as oral medication for chronic diarrhea. It consists of multiple herbs that originated from Song Dynasty in ancient China [15]. On the other hand, Liupao tea, a type of dark tea, is reported to be capable of treating gastrointestinal tract diseases. The great potential of antioxidants from dark teas can be used as functional ingredients in food products [16]. Liupao tea originates from Guangxi province, China. Liiupao tea has various benefits such as hypoglycemia, hypolipidemia, the modulation of gastrointestinal function, and microbial homeostasis [17]. The long-term consumption of Liupao tea has a sustainable effect on a person's fitness. Since we have quantified and qualified the main components of Liupao tea [18], we plan to analyze the chemical components inside Liupao tea using ultra-high performance liquid chromatography and quadrupole time of flight tandem mass spectrometry (UPLC-QTOF-MS/MS).

Several studies have highlighted the fact that Liupao tea play a beneficial role in relieving HFD-induced diabetes [19,20] and improving gastrointestinal function [17]; however, these reports mainly focused on one specific symptom and have not provided enough evidence for the potentially protective mechanism of Liupao tea against complex and multifaceted diseases. Therefore, the objectives of the present study were as follows: (1) identify the main components of Liupao tea; (2) estimate the effects of Liupao tea on gastrointestinal function, pro-inflammatory cytokines and water metabolism; (3) clarify the effects of Liupao tea on gut microbiota; (4) elucidate the potential mechanism of Liupao tea against IBS.

2. Materials and methods

2.1. Chemical reagents

Wuzhou Liupao tea was sourced from Wuzhou tea factory (Zhuang Autonomous Region, Guangxi, China). The Huoxiang Zhengqi oral liquid was purchased from MINJI Pharmaceutical Co., Ltd (Jiangxi, China). Lard oil was bought from GLOD GIFT FOOD Co., Ltd (Zhejiang, China). EDTA (pH 9.0) antigen repair solution, PBS buffer (pH 7.4), BSA solution, neutral balsam, TNF-α, IL-6, IL-1β, goat anti-rabbit IgG, goat anti-mouse IgG, and the DAB chromogenic kit were purchased from Service-Bio Co., Ltd (Wuhan, China). Ethanol and xylene were acquired from Sinopharm Chemical Reagent Co., Ltd (Shanghai, China).

2.2. Preparation of tea extracts

First, a 500 g sample of Liupao tea leaves was soaked together in a 10-fold volume (w/v) of distilled water for 1 h, heated to the boiling point, and maintained at 100 °C for 1 h. The residue was extracted twice. The mixed extracts were combined and concentrated using a rotatory evaporator. The extract was frozen for drying, and 177.26 g of tea extracts were obtained, with a yield ratio of 35.45%. Tea extracts were stored at −20 °C for use.

2.3. Chemical characterization by UPLC-QTOF-MS/MS

Liupao tea was prepared for chemical analysis according to Joo et al. [21] with modifications. The freeze-dried powder was

weighed accurately to 1.0 mg. It was loaded into a 10 mL volumetric flask and dissolved with 25% acetonitrile solution. The volume was adjusted to the appropriate tick mark. The sample was mixed and then filtered through a 0.22 μm microporous membrane to obtain the test solution before UPLC-QTOF-MS/MS analysis. A Thermo Accucore C18 column (100 × 2.1 mm, 2.6 μm, Thermo, USA) was used for chromatography, eluting with a mixture of 0.1% formic acid-aqueous solution (solvent A) and 0.1% formic acid-acetonitrile solution (solvent B). Elution was performed at 0.3 mL/min and the column temperature was set at 30 °C. The gradient elution was 0–1 min, 95% A; 1–5 min, 90-80% A; 5–9 min, 80-75% A; 9–15 min, 75-65% A; 15–18 min, 65-45% A; 18–22 min, 45-20% A; 22–30 min, 20-10% A. The injection volume was 1 μL. Mass spectra were registered at an interval of ESI negative and positive ion modes in a scan range of *m/z* 100–1500. The parameters in the ion mode were as follows: source voltage 3.5 kV, sheath gas pressure 35 psi, auxiliary gas pressure 10 psi, capillary temperature 320 °C, auxiliary gas temperature 350 °C. The scan mode was set as follows: full MS resolution 700000, dd-MS2 resolution 17500, MS/MS collision energy NCE 20, 40, and 60 eV. Data acquisition and processing were carried out with Xcalibur 4.1 and Thermo Compound Discoverer 3.1 software (Thermo Fisher Scientific, USA) to identify and retrieve the chemical compounds. It suggested the molecular formula based on the elemental composition of the parent mass ion. A search of the major fragment ions in the MS and MS/MS spectra of potential chemical compounds was performed using the MASS bank (http://www.massbank.jp/).

2.4. Animals and design

Specific-pathogen-free rats (180 ± 20 g) were purchased from the Laboratory Animal Center of Sun Yat-sen University, Guangzhou, China (SCXK (yue) 2017-0125). The animal studies were approved by the Committee on Laboratory Animal Care and Use of Guangdong Pharmaceutical University, Guangzhou, China (SYXK (yue) 2018-0002). After three days of adaptation, 48 rats were randomly divided into six groups: (1) normal (n = 8, N); (2) model (n = 8, M); (3) natural recovery (n = 8, NR); (4) Huoxiang Zhengqi oral liquid (n = 8, 1 mL/100 g, HOL); (5) low dose of Liupao tea (n = 8, 0.126 g tea leaves/100g, L-LPT); (6) high dose of Liupao tea (n = 8, 0.252 g tea leaves/100g, H-LPT).

Except for the N group, the rats in all groups were transferred to handmade cages (temperature: 18–25 °C, humidity 90% ± 5%) and placed in water (to a depth of 4 cm) every day from 8:00 to 16:00 for sustained cold exposure. The rats in each group were fasted and fed with 2 mL of cold water (4 °C) via gavage and then treated with 4 mL of cooked lard oil the following day for intermittent cold exposure. Rats in the L-LPT, H-LPT, and HOL groups were treated with tea extracts while saline was given to those in the M, NR, and N groups (days 1–45). Animal model construction for rats in the NR group ended on day 45. Modeling procedures in the N, M, L-LPT, H-LPT, and HOL groups continued. The open-field experiment was performed on day 55, after which the rats were sacrificed and samples were collected on day 60. The flow chart of animal experiment was shown in Fig. 1.

2.5. The open-field test

The rats were caressed consecutively for three days before the experiment. The central part consisted of a colorful picture. The rats were placed in the right corner of the test apparatus and a video was recorded for 5 min using a video camera. The arena was cleaned at intervals. All video tapes were analyzed by the principal investigator.

2.6. Determination of gastrointestinal function-related indicators

The body weight was recorded and feces samples were collected from each rat before sacrifice. A semi-solid meal was prepared as previously described [22]. Half an hour before dissection, the rats were administered a semi-solid paste (1 mL/100 g) via gavage. Then, the abdominal cavity of each rat was opened and the cardiac sphincter and distal pylorus were ligated to obtain the stomach. Gastrointestinal function-related indicators, including the gastric emptying rate, fecal water content, and intestinal water content,

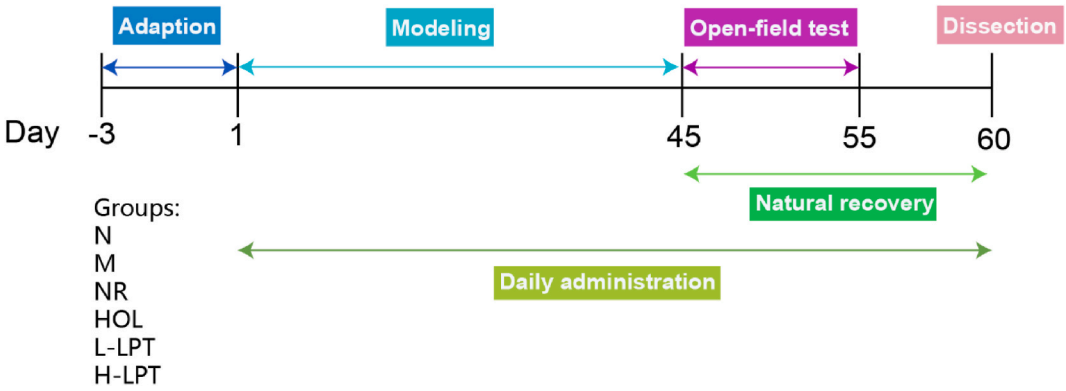

Fig. 1. Animal design. N, normal; M, model; NR, natural recovery group; HOL, Huoxiang Zhengqi oral liquid; L-LPT, low dose of Liupao tea; H-LPT, high dose of Liupao tea.

were measured and slightly modified per published articles [23,24].

2.7. Hematoxylin-eosin and immunohistochemical staining

HE staining was conducted. The distal colon section was segregated (the adjacent, proximal colon) as previously described [25]. After the distal colon, gastric, and renal sections were dissected, they were fixed with 4% paraformaldehyde overnight. Subsequently, the sections were washed with saline, immediately fixed with 4% paraformaldehyde, and dehydrated with alcohol for 12 h. Then, sections were incubated with dimethyl benzene and waxed with parafilm. Finally, the slides were re-stained with hematoxylin and eosin, and the HE staining procedure was completed.

IHC staining was performed. The embedded paraffin colon sections were dried for 10 min. The sections were deparaffinized in xylene, rehydrated in a graded alcohol series, and heated moderately for 8 min in EDTA solution (pH 9.0) for antigen retrieval. The heat was preserved for 8 min and again for 7 min. After cooling them down, segments were treated with PBS solution and washed with a decoloring shaker three times (5 min each). The endogenous peroxidase was quenched by 3% H_2O_2 at room temperature and incubated in dark for 25 min. Slices were treated with PBS solution (pH 7.4) and washed three times. The specific binding sections were blocked for 30 min using 3% BSA solution. The sections were incubated overnight with antigens, including TNF-α (1: 100), IL-6 (1: 800), IL-1β (1: 1000), and AQP3 (1: 2000). The procedure of adding PBS (pH 7.4) was conducted as described above. The sections were inoculated with goat anti-rabbit IgG (1:200) and goat anti-mouse IgG (1:200) and then incubated for 50 min. They were subjected to DAB color-rendering and then examined under a microscope. The sections were dehydrated in graded alcohol and rehydrated in xylene. These sections were dried, sealed with gum, and examined under a microscope, after which the images were acquired and analyzed.

2.8. Measurement of pro-inflammatory cytokines and AQP3

According to the positive areas of sections, the expression levels of TNF-α, IL-6, and IL-1β in gastrointestinal tissues were measured. The qualitative analysis of AQP3 in intestinal, gastric, and renal sections was performed using IHC staining images.

2.9. Serum sample measurements

The blood samples were collected from the abdominal vein and centrifuged (4000 r·min^{-1}, 5 min, 4 °C). The serum samples were stored at −80 °C. Gastrin (GAS), motilin (MTL), and D-lactic acid (D-LA) were measured per the manufacturer's protocols of the kit (Wuhan ColofulGene Biological Technology CO., Ltd, Wuhan, China). Triglyceride (TG), total cholesterol (TC), low-density lipoprotein (LDL), high-density lipoprotein (HDL), alanine transaminase (ALT), and uric acid (UA) levels were determined using an automatic biochemical analyzer offered by The First Affiliated Hospital/School of Clinical Medicine of Guangdong Pharmaceutical University (Guangzhou, China).

2.10. Real-time PCR and 16S rRNA sequencing analyses

Fecal samples were collected before sacrifice and stored at −80 °C. Per the manufacturer's instructions, fecal genomic DNA was extracted using the E. Z.N.A.® soil DNA Kit (Omega Bio-Tek, USA), qualified via 1% agarose gel electrophoresis, and quantified using the UV–vis spectrophotometer (NanoDrop 2000, Thermo Fisher Scientific, USA). The V3–V4 hypervariable regions of the bacteria 16SrRNA gene were amplified with primers 338F (5′ACTCCTACGGGAGGCAGCAG-3′) and 806R (5′-GGACTACHVGGGTWTCTAAT-3′) using a polymerase chain reaction (PCR) system (ABI GeneAmp® 9700, ABI, USA). Amplicons were then purified by gel extraction (Axygen Biosciences, Axygen, USA), quantified using QuantiFluor-ST (Promega, USA), pooled in equimolar concentrations, and paired-end sequenced using an Illumina MiSeq instrument (Illumina, USA). Then, libraries were generated and sequenced as previously described [26].

2.11. Bioinformatics analysis

Bioinformatics analyses were performed as described in a previous study [27] with slight modifications. PE reads (paired-end reads) obtained via Miseq sequencing were spliced according to the overlapping relationship. Operational Taxonomic Units (OTU) clustering analyses were performed using UPARSE (version 7.0, http://drive5.com/uparse/) based on similar value no less than 97%. All optimized sequences were mapped to the representative OTU sequences and OTUs were described using Venn diagrams. Then, the species of each sequence were classified using the RDP classifier (version 2.11) and compared with the Silva database (version 132). α-Diversity and β-diversity were performed using mothur software and R language tool. The consequent β-diversity consists of a principal component analysis (PCA) revealing different microbiota structures among the groups. Species variation was analyzed using R language and Python to estimate the significant impact of each species' abundance between the N and M group. The microbial function pathway was predicted through the phylogenetic investigation of communities via the reconstruction of unobserved states (PICRUSt) according to the Kyoto Encyclopedia of Genes and Genomes (KEGG) pathway. The R language tool was utilized to draw heatmaps.

2.12. Statistical analysis

Continuous data were expressed as the mean ± SEM. *P*-values were calculated using the one-way analysis of variance (AVONA) followed by the LSD method. We considered $p > 0.05$ to be statistically significant. All analyses were performed using SPSS 26 (SPSS Inc., San Francisco, USA) and figures were drawn using GraphPad Prism 8 (GraphPad software, California, USA).

3. Results

3.1. Chemical characterization of Liupao tea

To identify the chemical constituents of LPT, UPLC-QTOF-MS/MS was employed. Based on authentic compounds, available literature data and the obtained MS data, a total of 89 chemical components were tentatively identified, including catechins and their derivates, flavones and their glycosides, phenolic acids, amino acids, phenylpropanoids, polysaccharides, and caffeine. The total ion chromatograms (TIC) of LPT in both the positive and negative ion modes are displayed in Fig. 2. The data of the characterized compounds is presented in Table 1. Phenolic acids, catechins, caffeine and flavones were identified in LPT; more specifically, six compounds were detected, such as gallic acid, ellagic acid, (−)-epigallocatechin gallate (EGCG), caffeine, (−)-epicatechin gallate (ECG) and rutin. The contents of these components were shown in Table S1.

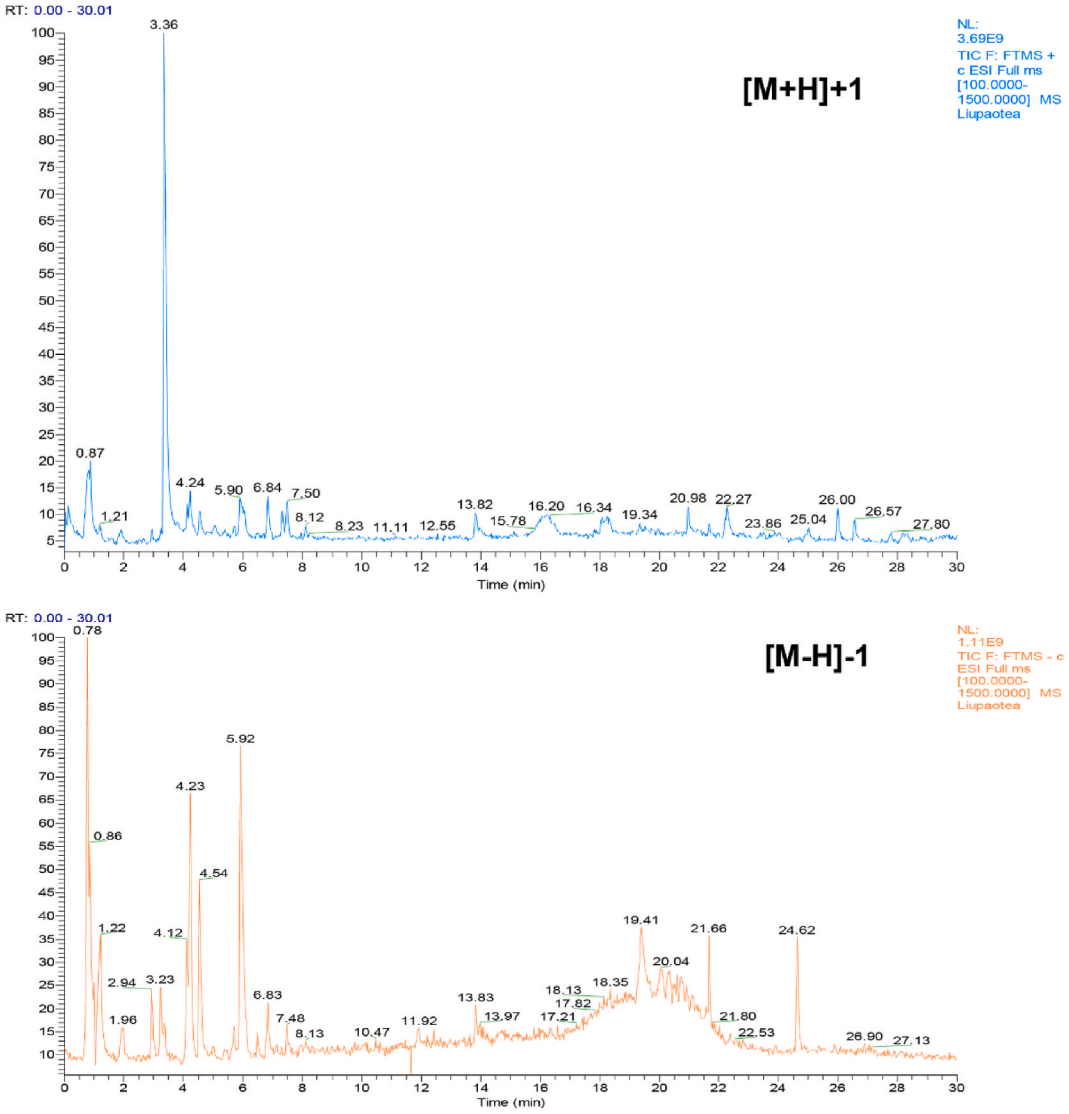

Fig. 2. Total ion chromatogram (TIC) obtained from UPLC-QTOF-MS analysis. (A) Positive mode. (B) Negative mode.

Table 1
Characterization results in UPLC-QTOF-MS/MS analysis.

No.	RT (min)	Compound Name	Ion	*m/z*	Formula	CAS
1	0.748	Choline	[M+H]+1	104.11	$C_5H_{13}NO$	62-49-7
2	0.772	Proline	[M+H]+1	116.07	$C_5H_9NO_2$	147-85-3
3	0.775	D-(−)-Quinic acid	[M − H]-1	191.06	$C_7H_{12}O_6$	77-95-2
4	0.78	Valine	[M+H]+1	118.09	$C_5H_{11}NO_2$	72-18-4
5	0.791	Guanine	[M+H]+1	152.06	$C_5H_5N_5O$	73-40-5
6	0.794	Uridine monophosphate	[M − H]-1	323.03	$C_9H_{13}N_2O_9P$	58-97-9
7	0.802	Adenosine 5'-monophosphate	[M − H]-1	346.06	$C_{10}H_{14}N_5O_7P$	61-19-8
8	0.814	DL-Malic acid	[M − H]-1	133.01	$C_4H_6O_5$	6915-15-7
9	0.826	*N*-Acetylornithine	[M+H]+1	175.11	$C_7H_{14}N_2O_3$	6205-08-9
10	0.827	*N*-Acetylornithine	[M − H]-1	173.09	$C_7H_{14}N_2O_3$	6205-08-9
11	0.866	Citric acid	[M − H]-1	191.02	$C_6H_8O_7$	77-92-9
12	0.874	Leucylproline	[M+H]+1	229.16	$C_{11}H_{20}N_2O_3$	6403-35-6
13	0.876	4-Oxoproline	[M − H]-1	128.03	$C_5H_7NO_3$	4347-18-6
14	0.877	L-Pyroglutamic acid	[M+H]+1	130.05	$C_5H_7NO_3$	98-79-3
15	0.877	Adenosine	[M+H]+1	268.1	$C_{10}H_{13}N_5O_4$	58-61-7
16	0.885	6-Aminocaproic acid	[M+H]+1	132.1	$C_6H_{13}NO_2$	60-32-2
17	1.173	3-Methylxanthine	[M+H]+1	167.06	$C_6H_6N_4O_2$	1076-22-8
18	1.213	Pyrogallol	[M − H]-1	125.02	$C_6H_6O_3$	87-66-1
19	1.214	Gallic acid[a]	[M − H]-1	169.01	$C_7H_6O_5$	149-91-7
20	1.514	DL-Leucineamide	[M+H]+1	131.12	$C_6H_{14}N_2O$	33042-97-6
21	1.609	L-Tyrosine	[M+H]+1	182.08	$C_9H_{11}NO_3$	60-18-4
22	1.886	Theobromine	[M+H]+1	181.07	$C_7H_8N_4O_2$	83-67-0
23	2.13	Gentisic acid	[M − H]-1	153.02	$C_7H_6O_4$	490-79-9
24	2.507	Paraxanthine	[M+H]+1	181.07	$C_7H_8N_4O_2$	611-59-6
25	2.659	*trans*-3-Indoleacrylic acid	[M+H]+1	188.07	$C_{11}H_9NO_2$	1204-06-4
26	3.124	2-Isopropylmalic acid	[M − H]-1	175.06	$C_7H_{12}O_5$	3237-44-3
27	3.19	Methyl gallate	[M − H]-1	183.03	$C_8H_8O_5$	99-24-1
28	3.246	Catechin	[M − H]-1	289.07	$C_{15}H_{14}O_6$	154-23-4
29	3.368	3-Pyridylamidoxime	[M+H]+1	138.07	$C_6H_7N_3O$	1594-58-7
30	3.369	Caffeine[a]	[M+H]+1	195.09	$C_8H_{10}N_4O_2$	58-08-2
31	3.453	Neochlorogenic acid	[M − H]-1	353.09	$C_{16}H_{18}O_9$	906-33-2
32	4.132	3,4-Dihydroxybenzaldehyde	[M+H]+1	139.04	$C_7H_6O_3$	139-85-5
33	4.212	2-Hydroxycinnamic acid	[M+H]+1	147.04	$C_9H_8O_3$	614-60-8
34	4.546	4-Hydroxybenzoic acid	[M+H]+1	139.04	$C_7H_6O_3$	99-96-7
35	4.549	(−)-Epigallocatechin gallate (EGCG)[a]	[M − H]-1	457.08	$C_{22}H_{18}O_{11}$	989-51-5
36	5.017	myricetin 3-O-beta-D-galactopyranoside	[M − H]-1	479.08	$C_{21}H_{20}O_{13}$	15648-86-9
37	5.021	Myricetin	[M+H]+1	319.05	$C_{15}H_{10}O_8$	529-44-2
38	5.07	Boldenone undecylenate	[M+H]+1	453.34	$C_{30}H_{44}O_3$	13103-34-9
39	5.12	*N*-Acetyl-L-phenylalanine	[M − H]-1	206.08	$C_{11}H_{13}NO_3$	2018-61-3
40	5.387	Kaempferol 3-O-Rhamnoside	[M − H]-1	739.21	$C_{33}H_{40}O_{19}$	83170-31-4
41	5.624	5-[(benzoyloxy)methyl]-4,5,6-trihydroxycyclohex-2-en-1-yl benzoate	[M+H]+1	402.16	$C_{21}H_{20}O_7$	78804-17-8
42	5.64	Ellagic acid[a]	[M − H]-1	301	$C_{14}H_6O_8$	476-66-4
43	5.698	Rutin[a]	[M − H]-1	609.15	$C_{27}H_{30}O_{16}$	153-18-4
44	5.836	Quercetin-3β-D-glucoside	[M − H]-1	463.09	$C_{21}H_{20}O_{12}$	482-35-9
45	5.916	4-Hydroxybenzaldehyde	[M+H]+1	123.04	$C_7H_6O_2$	123-08-0
46	5.919	*N*-Isovalerylglycine	[M − H]-1	158.08	$C_7H_{13}NO_3$	16284-60-9
47	5.921	(−)-Epicatechin gallate (ECG)[a]	[M − H]-1	441.08	$C_{22}H_{18}O_{10}$	1257-08-5
48	5.978	Myricitrin	[M − H]-1	463.09	$C_{21}H_{20}O_{12}$	17912-87-7
49	6.119	Kaempferitrin	[M − H]-1	577.16	$C_{27}H_{30}O_{14}$	482-38-2
50	6.484	Trifolin	[M+H]+1	449.11	$C_{21}H_{20}O_{11}$	23627-87-4
51	6.793	Luteolin	[M+H]+1	287.06	$C_{15}H_{10}O_6$	491-70-3
52	6.853	Quercetin	[M+H]+1	303.05	$C_{15}H_{10}O_7$	117-39-5
53	7.18	4-Hydroxybenzoic acid	[M − H]-1	137.02	$C_7H_6O_3$	99-96-7
54	7.322	Triethyl phosphate	[M+H]+1	183.08	$C_6H_{15}O_4P$	78-40-0
55	7.323	Diethyl phosphate	[M+H]+1	155.05	$C_4H_{11}O_4P$	598-02-7
56	7.833	Quercetin	[M − H]-1	301.04	$C_{15}H_{10}O_7$	117-39-5
57	7.955	Kaempferol	[M+H]+1	287.06	$C_{15}H_{10}O_6$	520-18-3
58	11.523	12-Aminododecanoic acid	[M+H]+1	216.2	$C_{12}H_{25}NO_2$	693-57-2
59	14.044	*N*,N-Dimethyldecylamine *N*-oxide	[M+H]+1	202.22	$C_{12}H_{27}NO$	2605-79-0
60	15.116	2,2,6,6-Tetramethyl-4-piperidinol	[M+H]+1	158.15	$C_9H_{19}NO$	2403-88-5
61	17.196	6-(3-Pyridyl)-1,3,5-triazine-2,4-diamine	[M+H]+1	189.09	$C_8H_8N_6$	18020-61-6
62	18.072	Palmitic acid	[M+H]+1	274.27	$C_{16}H_{32}O_2$	57-10-3
63	18.224	2-Amino-1,3,4-octadecanetriol	[M+H]+1	318.3	$C_{18}H_{39}NO_3$	13552-11-9
64	18.226	Sedanolide	[M+H]+1	195.14	$C_{12}H_{18}O_2$	6415-59-4
65	18.246	Decanamide	[M+H]+1	172.17	$C_{10}H_{21}NO$	2319-29-1
66	19.288	Ostruthin	[M − H]-1	297.15	$C_{19}H_{22}O_3$	148-83-4
67	19.405	Dodecyl sulfate	[M − H]-1	265.15	$C_{12}H_{26}O_4S$	151-41-7

(*continued on next page*)

Table 1 (*continued*)

No.	RT (min)	Compound Name	Ion	*m/z*	Formula	CAS
68	19.458	Bis(4-ethylbenzylidene)sorbitol	[M+H]+1	415.21	$C_{24}H_{30}O_6$	79072-96-1
69	19.566	4-Ethoxy ethylbenzoate	[M+H]+1	195.1	$C_{11}H_{14}O_3$	23676-09-7
70	19.963	Diphenylamine	[M+H]+1	170.1	$C_{12}H_{11}N$	122-39-4
71	20.769	4-Dodecylbenzenesulfonic acid	[M − H]-1	325.18	$C_{18}H_{30}O_3S$	121-65-3
72	20.772	Cyclohexyl phenyl ketone	[M+H]+1	189.13	$C_{13}H_{16}O$	712-50-5
73	21.101	Myristyl sulfate	[M − H]-1	293.18	$C_{14}H_{30}O_4S$	4754-44-3
74	21.254	3,5-di-*tert*-Butyl-4-hydroxybenzaldehyde	[M+H]+1	235.17	$C_{15}H_{22}O_2$	1620-98-0
75	21.801	Tris (2-butoxyethyl) phosphate	[M+H]+1	399.25	$C_{18}H_{39}O_7P$	78-51-3
76	22.271	Diisobutylphthalate	[M+H]+1	279.16	$C_{16}H_{22}O_4$	84-69-5
77	23.416	16-Hydroxyhexadecanoic acid	[M − H]-1	271.23	$C_{16}H_{32}O_3$	506-13-8
78	23.547	7-(2-hydroxypropan-2-yl)-1,4a-dimethyl-decahydronaphthalen-1-ol	[M+H]+1	223.21	$C_{15}H_{28}O_2$	60132-35-6
79	23.639	Palmitoyl ethanolamide	[M+H]+1	300.29	$C_{18}H_{37}NO_2$	544-31-0
80	24.41	Estriol	[M+H]+1	311.16	$C_{18}H_{24}O_3$	50-27-1
81	24.631	2,2'-Methylenebis (4-methyl-6-*tert*-butylphenol)	[M − H]-1	339.23	$C_{23}H_{32}O_2$	119-47-1
82	24.912	Hexadecanamide	[M+H]+1	256.26	$C_{16}H_{33}NO$	629-54-9
83	25.334	Oleamide	[M+H]+1	282.28	$C_{18}H_{35}NO$	301-02-0
84	25.793	Oleoyl ethanolamide	[M+H]+1	308.3	$C_{20}H_{39}NO_2$	111-58-0
85	26.567	Laurolactam	[M+H]+1	198.19	$C_{12}H_{23}NO$	947-04-6
86	26.619	Erucamide	[M+H]+1	338.34	$C_{22}H_{43}NO$	112-84-5
87	27.025	Diethyl 2-{[(2-{[3-(trifluoromethyl)-2-pyridyl]amino}ethyl)amino]methylidene} malonate	[M − H]-1	374.13	$C_{16}H_{20}F_3N_3O_4$	215500-77-9
88	28.177	Stearamide	[M+H]+1	284.3	$C_{18}H_{37}NO$	124-26-5
89	28.209	Stearoyl Ethanolamide	[M+H]+1	310.31	$C_{20}H_{41}NO_2$	111-57-9

[a] This letter indicates the identification of the compound was confirmed by the authentic standards.

3.2. Effects of Liupao tea on locomotor activity (open-field test) and body weight

The rats in the N group were in good shape, had shiny fur, and were more active during the test (Fig. 3A). However, rats with IBS had gloomy fur and showed less exploratory behaviors. Rats in the M group acted more slowly, preferred to stay on the verge of the arena, and expressed less desire for explorations compared to those in the N group (Fig. 3B). The mean body weight of rats in the M group (247.34 g) was lower than that in all the other groups (Fig. 3C), while the locomotive velocity in the H-LPT group (13.13 mm/s) was higher than that in the other groups (Fig. 3D).

3.3. Effects of Liupao tea on spleen coefficient and liver coefficient

The spleen coefficient (SC) in the L-LPT group (2.27 mg/g) was higher than that in the M group (1.91 mg/g) ($p < 0.05$) (Fig. 3E).

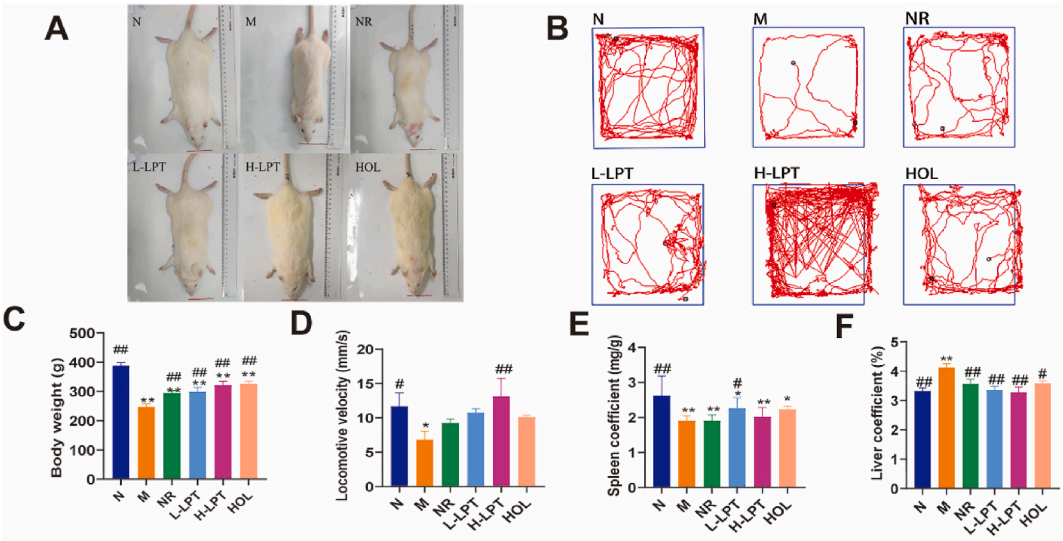

Fig. 3. Locomotor activity and body informatics. (A) The length of body. (B) Track maps of the open-field test. (C) Body weight. (D) Locomotive velocity. (E) Spleen coefficient. (F) Liver coefficient. Data are expressed as the mean ± SEM. *p < 0.05, **$p < 0.01$ versus the N group; #$p < 0.05$, ##$p < 0.01$ versus the M group.

However, L-LPT and H-LPT administration significantly decreased the liver coefficient (both $p < 0.01$) (Fig. 3F).

3.4. Effects of Liupao tea on gastrointestinal function

Gastrointestinal function-related parameters were measured. The gastric emptying rate in the M group (162.75%) was approximately 1.9-fold that in the N group (84.92%) ($p < 0.05$) (Fig. 4A), and there was a significant difference in this parameter between drug treatment groups and the M group ($p < 0.01$). However, there was no significant difference in this parameter between the NR and M groups.

The fecal water content in the M group was 74.77%, which was higher than all the other groups (Fig. 4B). The content in the M group was 1.5-fold that in the HOL group (50.30%), 1.4-fold that in the L-LPT (52.17%), and 1.2-fold that in the H-LPT (63.76%). The contents in the N and NR groups were 48.83% and 68.47%, respectively.

The intestinal water content of rats in the M group was 86.15%, and treatment with L-LPT (79.21%) significantly decreased this intestinal water content (Fig. 4C). In the M group (86.15%), L-LPT (79.21%) and H-LPT (80.15%) had a significantly greater effect on the intestinal water content ($p < 0.01$) than HOL (80.54%) did ($p < 0.05$).

3.5. Effects of Liupao tea on the morphological damages of gastric, colon and renal tissues

Microscopic examinations of gastric tissues demonstrated that rat colons in the N group had undamaged walls and intact morphologies (Fig. 5A). Its epithelial mucosa was arranged regularly. After modeling, the mucosal epithelial erosion was obvious and the colonic mucosa was congested with inflammatory cells infiltration and aggregation were observed in the mucosa, which may be defined as superficial gastritis. Glandular atrophy was observed and glands even disappeared in the lamina propria of the colon. The mucosal membrane was thinner and the submucosal vessels were congested. Compared to the M group, the epithelial mucosa in the NR group showed a tendency towards degeneration and necrosis. Its epithelial cells were arranged irregularly and there was some inflammatory cell infiltration. Although the overall epithelial mucosa in the L-LPT group was arranged regularly, minimal inflammatory cell infiltration could be observed. The epithelial mucosa in gastric tissues of the H-LPT group was basically restored to a regular shape, and the other obvious pathological states were reversed.

We also observed the colonic morphological structure. Epithelial mucosal cells in the N group were arranged in order (Fig. 5B). However, histopathological observations on colonic segments included diffusing degeneration and necrosis of epithelial serosa, the sparseness of the colonic mucosa, granulation tissue generation, inflammatory cell infiltration, glandular atrophy in the lamina propria of the colon, thinner submucosal structures, and significant edema. The same histopathological characteristics as the M group could be observed in the NR group. However, LPT administration had reversed the above symptoms to some extent. Glandular atrophy in the lamina propria and submucosal edema were slightly improved by L-LPT. All of the morphological damage was reversed by H-LPT.

The renal tissue sections were stained with HE (Fig. 5C). Pathological changes induced by HFD/CE in renal tissues were normalized by LPT and HOL administration.

3.6. Effects of Liupao tea on the expression of pro-inflammatory cytokines and AQP3

We assessed the positive area of pro-inflammatory cytokines, IL-6, IL-1β, and TNF-α in gastric and colonic sections using immunohistochemical methods. The levels of IL-6, IL-1β, and TNF-α increased in the gastric and colonic sections of colonic inflammatory rats while the LPT administration group showed lower levels of IL-6, IL-1β, and TNF-α (all $p < 0.01$) (Figs. 6 and 7). Furthermore, AQP3, as a cell membrane transporter, was detected. The mean level of AQP3 in the stomachs of rats in the L-LPT (1.16%) was three times less than that in the stomachs of those in the M group (2.31%) ($p < 0.01$) (Fig. 8A). As for the colonic part (Fig. 8B), the AQP3 mean level in the H-LPT group (31.26%) was 2.2 times higher than that in the M group (14.31%) ($p < 0.01$). The level of AQP3 increased in the renal

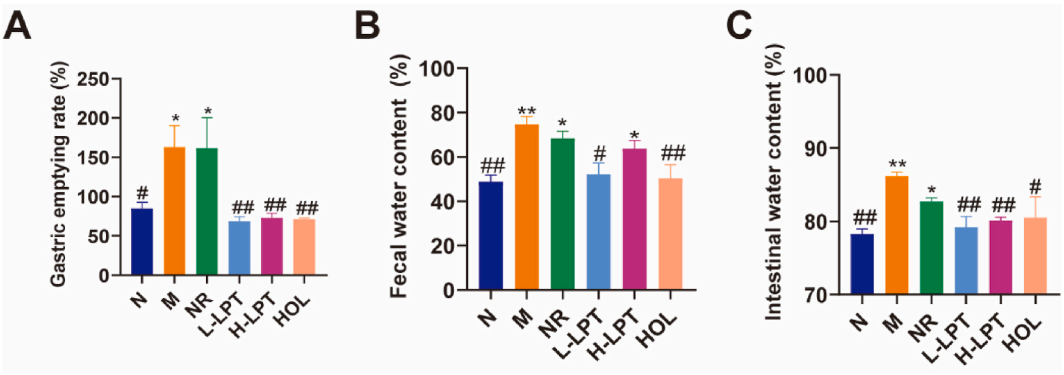

Fig. 4. Gastrointestinal function. (A) Gastric emptying rate. (B) Fecal water content. (C) Intestinal water content. Data are expressed as the mean ± SEM. $*p < 0.05$, $**p < 0.01$ versus the N group; $\#p < 0.05$, $\#\#p < 0.01$ versus the M group.

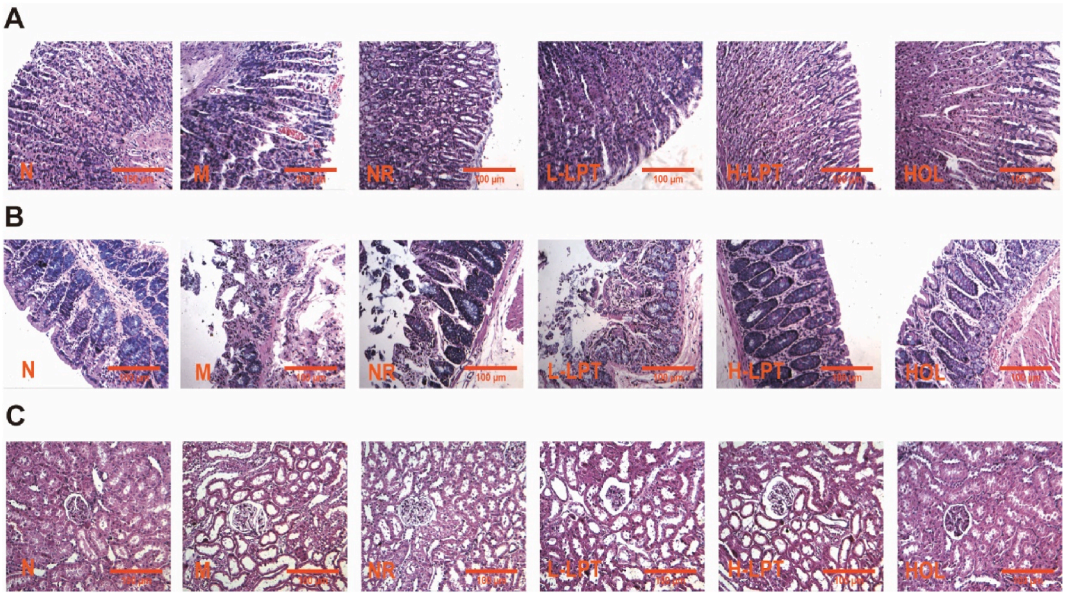

Fig. 5. Morphological damages. (A) Gastric tissues. (B) Colonic tissues. (C) Renal tissues.

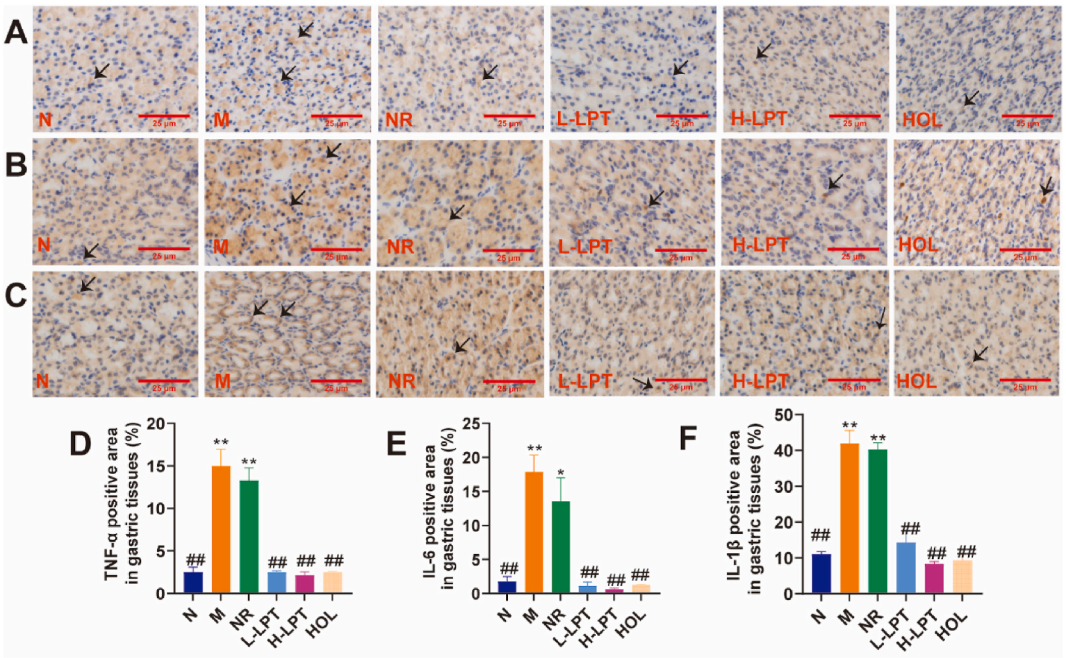

Fig. 6. Pro-inflammatory cytokines expression in gastric tissues. (A) IHC staining of TNF-α. (B) IHC staining of IL-6. (C) IHC staining of IL-1β. (D) TNF-α expression level. (E) IL-6 expression level. (F) IL-1β expression level. Arrows indicate brown-stained nuclei. Data are expressed as the mean ± SEM. $*p < 0.05$, $**p < 0.01$ versus the N group; $\#p < 0.05$, $\#\#p < 0.01$ versus the M group. (For interpretation of the references to color in this figure legend, the reader is referred to the Web version of this article.)

sections of rats in the M group (8.94%) compared to those in the N group (4.58%) ($p < 0.01$) while L-LPT and H-LPT administration was associated with less elevated levels of AQP3 (6.58% and 3.39%, respectively) (both $p < 0.01$) (Fig. 8C).

3.7. Effects of Liupao tea on serum metabolites

Levels of TC, LDL, TG, ALT, UA, and D-LA were higher in the M group than in the N group (all $p < 0.05$) (Fig. 9); however, MTL and

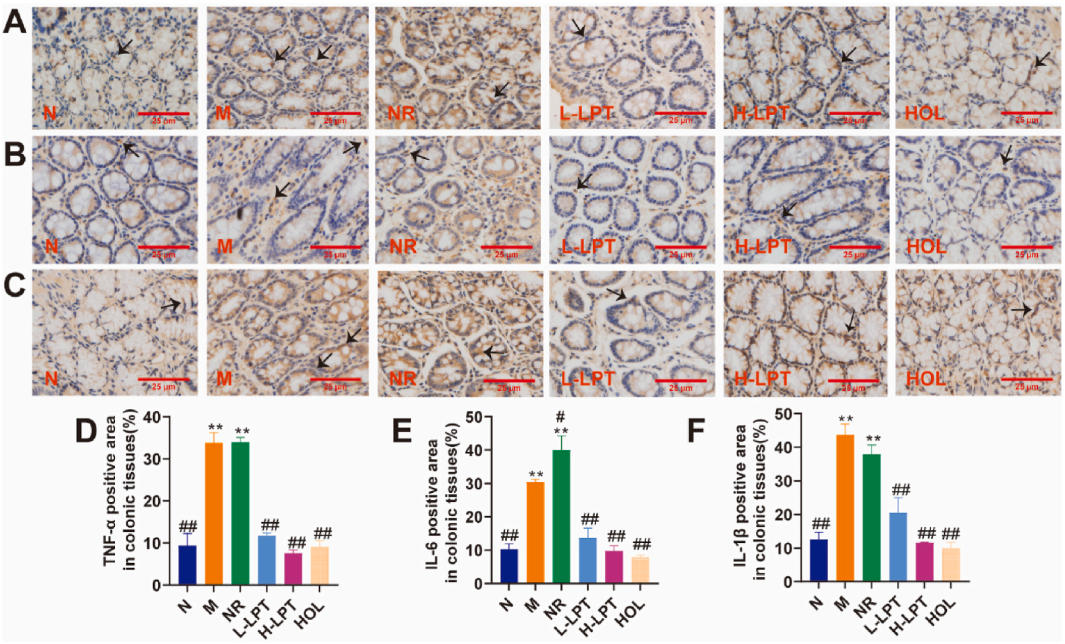

Fig. 7. Pro-inflammatory cytokines expression in colonic tissues. (A) IHC staining of TNF-α. (B) IHC staining of IL-6. (C) IHC staining of IL-1β. (D) TNF-α expression level. (E) IL-6 expression level. (F) IL-1β expression level. Arrows indicate brown-stained nuclei. Data are expressed as the mean ± SEM. $*p < 0.05$, $**p < 0.01$ versus the N group; $\#p < 0.05$, $\#\#p < 0.01$ versus the M group. (For interpretation of the references to color in this figure legend, the reader is referred to the Web version of this article.)

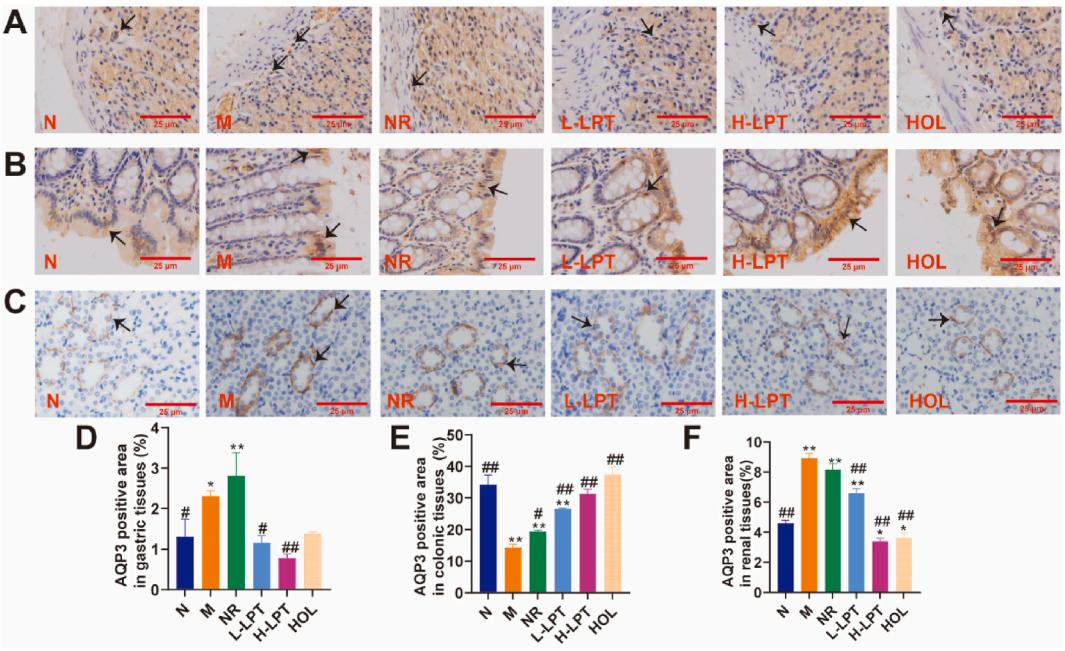

Fig. 8. AQP3 expression in gastric, colonic and renal tissues. (A) IHC staining of AQP3 in gastric tissues. (B) IHC staining of AQP3 in colonic tissues. (C) IHC staining of AQP3 in renal tissues. (D) AQP3 expression level in gastric tissues. (E) AQP3 expression level in colonic tissues. (F) AQP3 expression level in renal tissues. Arrows indicate brown-stained nuclei. Data are expressed as the mean ± SEM. $*p < 0.05$, $**p < 0.01$ versus the N group; $\#p < 0.05$, $\#\#p < 0.01$ versus the M group. (For interpretation of the references to color in this figure legend, the reader is referred to the Web version of this article.)

GAS levels in the M group were significantly lower than those in the N group ($p < 0.01$). The IBS-induced elevations in the levels of TC, LDL, TG, ALT, and UA were reversed by LPT treatment while LPT treatment upregulated MTL and GAS.

3.8. Effects of Liupao tea on the diversity and composition of gut microbiota

To assess the regulation of Liupao tea on gut microbiota, high-throughput sequencing was used to analyze and compare the gut microbiota. α-Diversity was featured as Chao 1 and Shannon indexes. The Chao1 and Shannon indexes were significantly reduced in colonic inflammatory rats but significantly reversed by LPT treatment. The Shannon indexes proved that OUT abundance in LPT groups was higher than that in the M group (Fig. 10A and B) and Chao1 showed a similar tendency (Fig. 10C). As the Venn diagram shows, the level of OUT was least among the groups; however, the intervention of Liupao tea increased OUT in rats with colonic inflammatory.

The Principal Component Analysis was applied to evaluate β-diversity among the samples. The sample points of the M group were assembled closely and clearly separated from those of the other groups (Fig. 10D), which indicated the success of the IBS animal model and microbial imbalance. As Fig. 10E–F shows, the OUT level in the M group was 844 and the number of unique species was 3, which

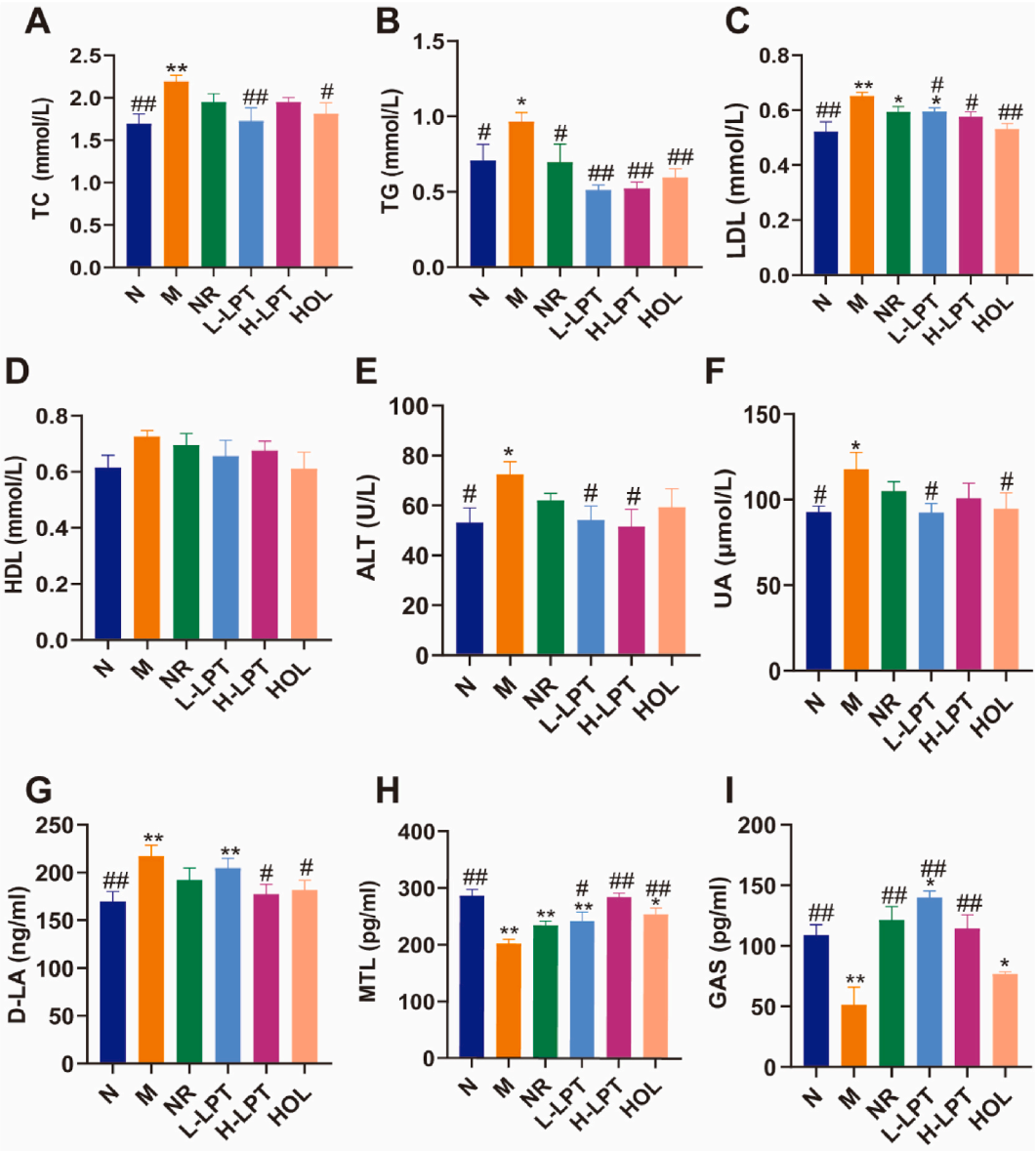

Fig. 9. Serum metabolites. (A) TC. (B) TG. (C)LDL. (D) HDL. (E) ALT. (F) UA. (G) D-LA. (H) MTL. (I) GAS. Data are expressed as the mean ± SEM. *$p < 0.05$, **$p < 0.01$ versus the N group; #$p < 0.05$, ##$p < 0.01$ versus the M group.

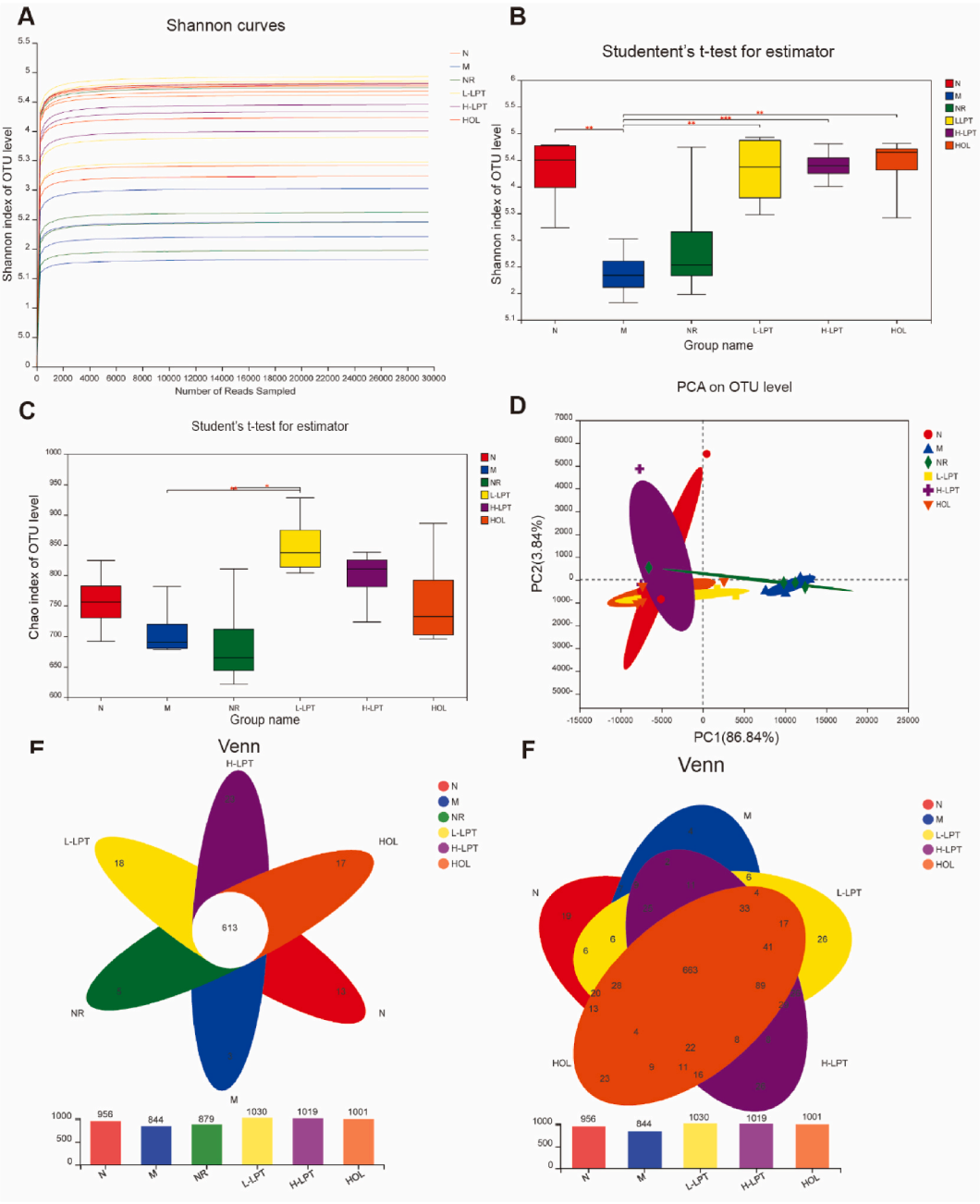

Fig. 10. Comparison of gut microbial diversity and composition between groups. (A) Shannon curves. (B) Shannon indexes of OTU level. (C) Chao indexes of OTU level. (D) PCA on OTU level. (E) and (F) Venn diagram of OTUs.

was the least among all the groups. The decrease in the diversity and abundance of microbiota was considered a sign of microbial imbalance. This implied a successful induction of HFD/CE. LPT and HOL intervention significantly reversed the reduction in microbial diversity and the abundance caused by HFD/CE induction.

3.9. Comparative analyses at the phylum and genus levels

The community abundance of the different groups at the phylum level can be seen in Fig. 11A. *Firmicutes*, *Bacteroidetes*, *Spirochaetes* and *Actinobacteria* were dominant in LPT groups while *Firmicutes* and *Bacteroidetes* were dominant in the M group. At the genus level, *Lacobacillus*, *norank_f_Muribaculaceae*, *Lachnospiraceae_NK4a163_group*, *unclassified_f_Lachnospiraceae*, *Alloprevotella*, and *Clostridium_sensu_stricto_1* had higher proportions in the LPT groups than in the M group (Fig. 11B). Microbiota diversity increased after LPT

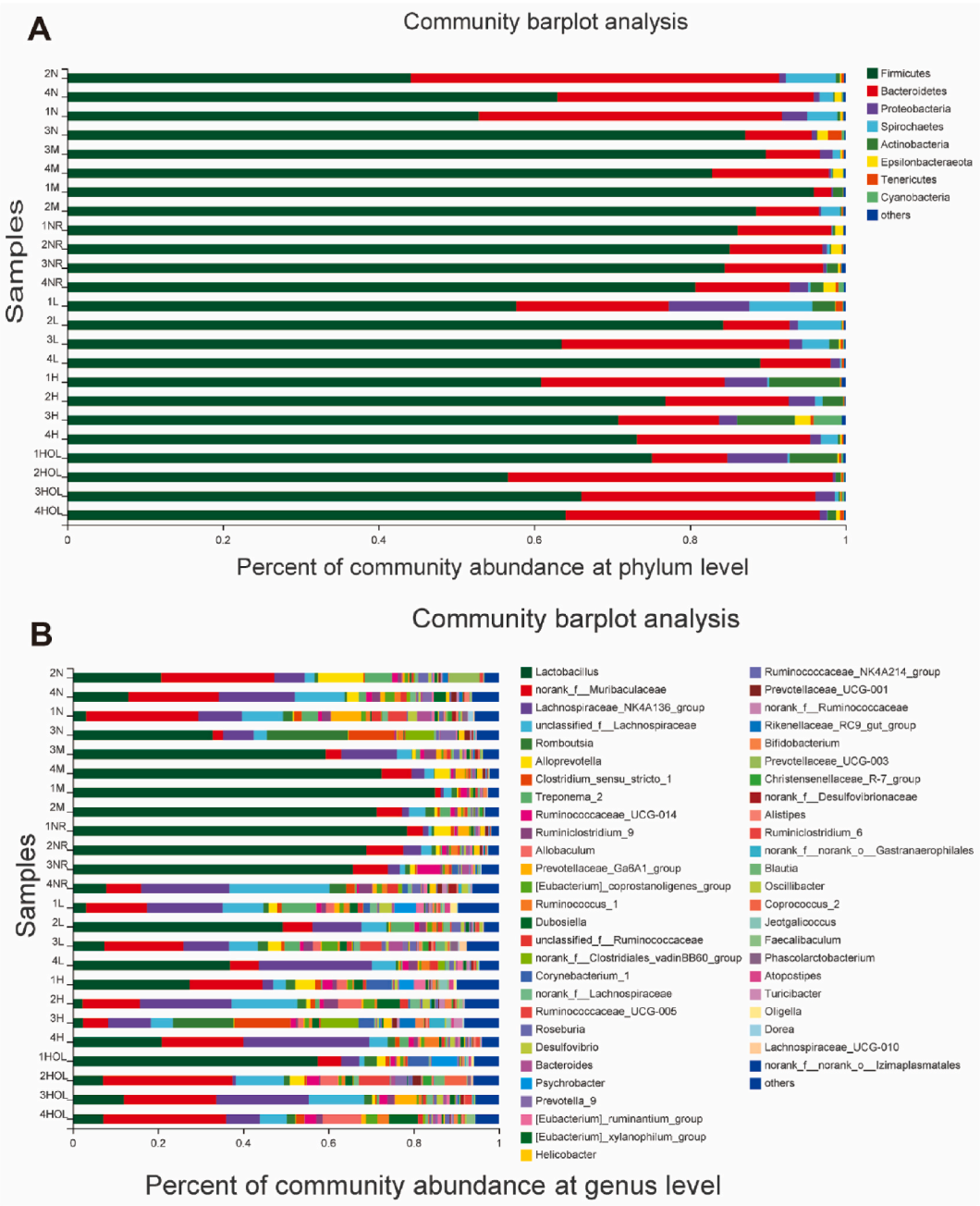

Fig. 11. Composition of the gut microbiota. (A) Column diagram of the microbial composition at the phylum level. (B) Column diagram of the microbial composition at the genus level.

treatment.

Student's t-test was used to verify the species' variation between the N and M groups. According to community abundance results (Fig. 12), the relative abundance of top-20 ranking bacteria was screened via Student's t-test bar plot analysis. Only at $p < 0.05$ could bacteria be considered biological markers. At the phylum level (Fig. 12A), the gut microbiota was primarily composed of *Firmicutes* and *Bacteroidetes*. HFD/CE induction significantly increased the abundance of *Firmicutes* ($p < 0.05$) and decreased that of *Bacteroidetes* ($p < 0.05$). Although there was no significant difference in the abundance of other bacteria, such as *Spirochaetes*, *Proteobaccteria*, *Epsilonbacteraeota* between the N and M group, they were screened for their higher abundance among bacteria. At the genus level (Fig. 12B), the genera with greater reductions in rats with IBS included *Muribaculaceae_f_norank, Ruminococcaceae_f_norank, Prevotellaceae_f_unclassified,* and *group_020fcs_Lachnospiraceae*.

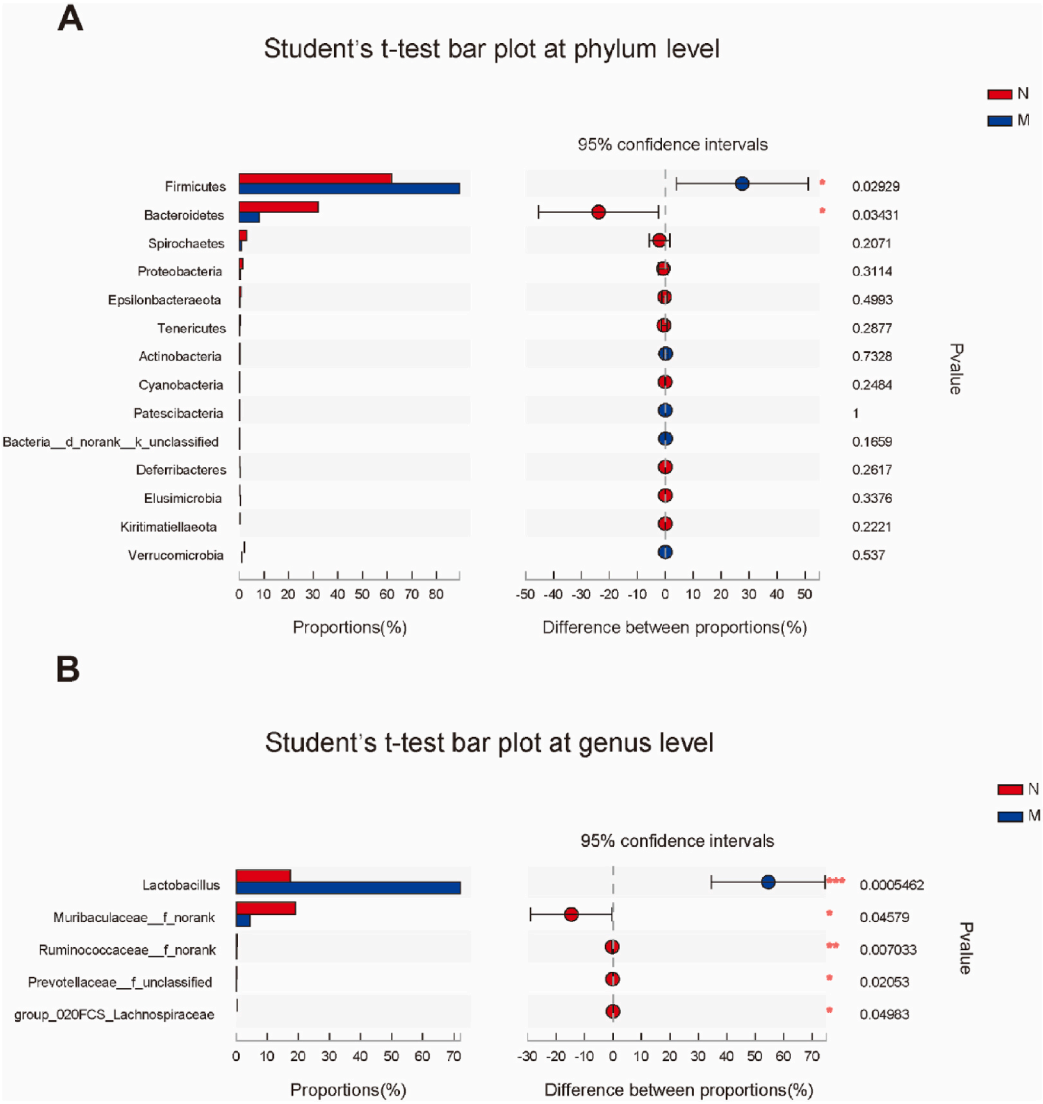

Fig. 12. Potential biological markers in rats with IBS. (A) Most abundant phyla in the N and M group. (B) Most abundant genera in the N and M groups. $*p < 0.05$, $**p < 0.01$, $***p < 0.001$ versus the N group.

3.10. Function prediction and relationship between physiological parameters and species

Cluster of Orthologous Groups of proteins (COG) function prediction analyses can predict the functional compositions between the N and M group of microbial communities in samples from amplicon sequencing results. Changes in lipid metabolism, amino acid metabolism, and other pathway functions were closely related to the pathogenesis of IBS ($p < 0.05$, Fig. 13A).

The relationship between the relative abundance of the top 20 genera and physicochemical parameters was analyzed via the Spearman analysis. At the genus level, most bacterial strains, such as *Bacteroides*, *Dubosiella*, *norank_f_Muribaculaceae*, *norank_f_Lachnospiraceae*, were positively correlated with the BD, LV, GAS and SC but negatively correlated with the GER, D-LA, ALT, TC, HLD, LDL, TG and UA (Fig. 13B). *Lactobacillus* and *unclassified_p_Firmicutes* showed the opposite correlation with these indexes, compared to most genera. At the phylum level, Firmicutes was negatively correlated with BS, LV, GAS and SC but positively correlated with the other indexes (Fig. 13C). *Bacteroidetes* showed the reverse correlation compared to *Firmicutes*.

To further clarify the correlation between the efficacy indicators measured in this experiment and the intestinal flora of the samples, the correlation between intestinal flora and the efficacy indicators was analyzed in this study, mainly based on the RDA and the correlation heatmap of environmental factors. The results of the RDA showed that the changes in all efficacy indexes were significantly correlated with the changes in the intestinal flora (Fig. 13D), among which the four indexes of blood lipids, the intestinal water content, D-LA, UA, ALT, and GER were significantly positively correlated with the intestinal flora of rats, and LDL had the strongest effect. The effects of BD, MTL, GAS, and LV on the intestinal flora of rats were significantly negatively correlated, and the

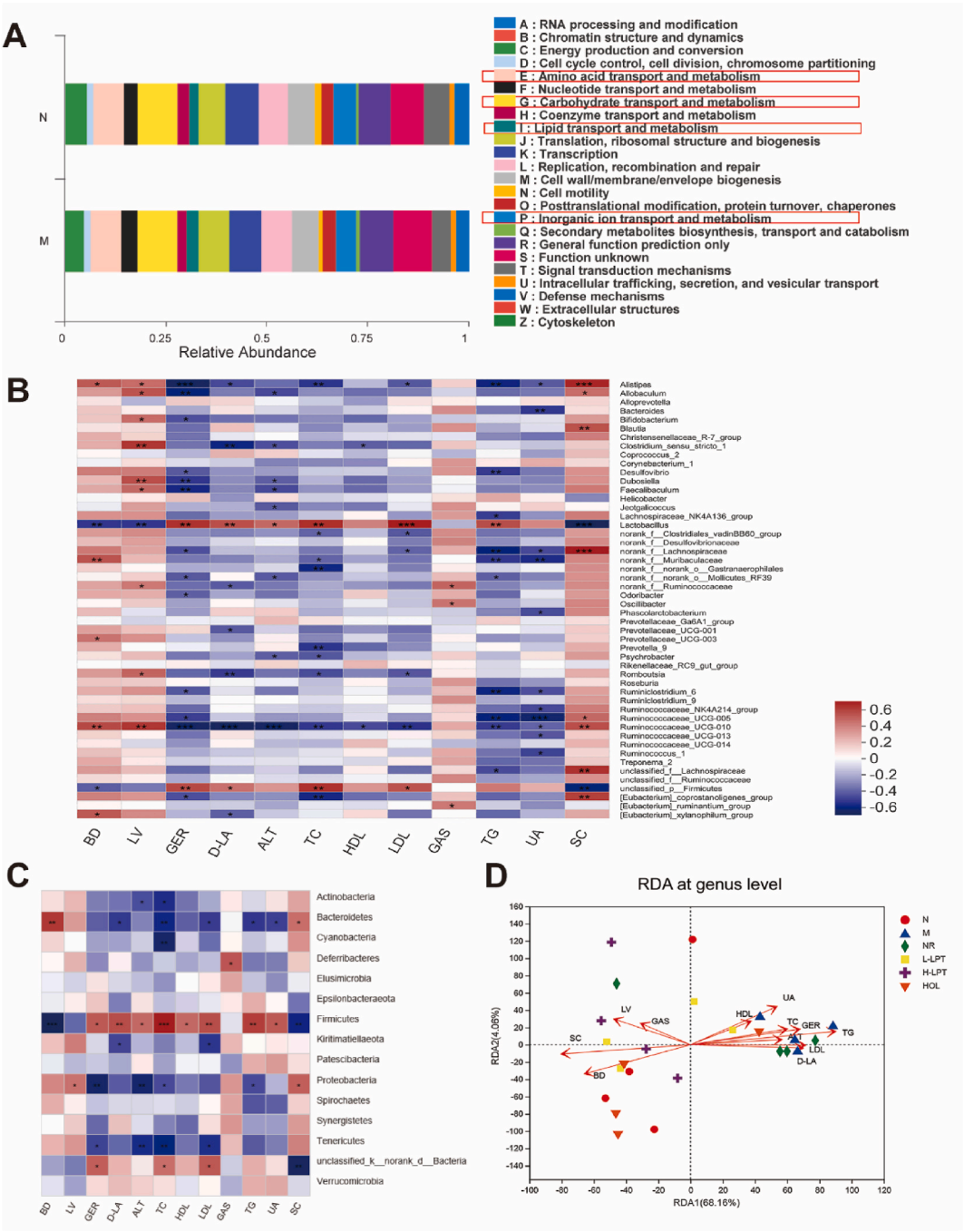

Fig. 13. Function prediction and the relationship between biological parameters and microbiota. (A) Comparison of COG functional categories between the N and M group. The red frames represent the most important functions. (B) Correlation between biological parameters and genera. (C) Correlation between biological parameters and phyla. Colors in gradual change show different degrees of relevance in (B) and (C). Rectangles in red indicate the positive relationships while those in blue indicate the negative relationships. (D) RDA between biological parameters and genera. The intersection angle between the arrow line segment and the axis indicates the correlation between indexes and bacteria. The small angle shows the positive correlation between indexes and bacteria. $*p < 0.05$, $**p < 0.01$, $***p < 0.001$ versus the N group. (For interpretation of the references to color in this figure legend, the reader is referred to the Web version of this article.)

effect of the body weight was the strongest.

4. Discussion

In recent years, intestinal health has gained increasing attention. We hope to find dietary modifications to maintain proper intestinal health. According to our previous studies [18], 11 batches of Liupao tea were qualified and quantified through HPLC fingerprints. LPT contains 1.86–25.91 mg/g of EGCG and 2.81–30.48 mg/g of ECG. In terms of flavones, rutin, gallic acid, and ellagic acid range from 5.75 to 14.34 mg/g, 5.06–14.13 mg/g, and 10.82–26.63 mg/g, respectively. There is a range of 56.24–82.30 mg/g of caffeine. All of these chemical components are biologically active in Liupao tea. Our team has previously quantified these six main components through UPLC-QTOF-MS/MS. Based on reported literature and database, more effective ingredients are identified in this study. It provides us with a chemical foundation to study the therapeutic properties of Liupao tea. The data demonstrate Liupao tea is rich in catechins, polyphenols, amino acids, caffeine, polysaccharides and other components.

According to the TCM view on the etiology of IBS, the invasion of evils (namely coldness, dampness, and heat) combined with the weakness of *Zang Fu* (specifically the spleen, stomach, and kidney) can be defined as irritable bowel syndrome [28]. Improper diet and emotional disorders lead to irritable bowel symptoms such as abdominal pain, bloating, diarrhea, and constipation. IBS not only alters the form and frequency of stool but also contributes to the stagnation of bowel dampness, which results in diarrhea. To avoid the adverse effects of chemical drugs, it would be worthwhile to use natural products to protect oneself from developing IBS. Liupao tea has the functions of relieving heat and dampness, invigorating the stomach and spleen [29], arousing considerable attention as an alternative treatment for treating IBS. We used the open-field test, gastrointestinal-related hormones, and its histopathological features to evaluate the effect of Liupao tea on IBS. After model construction, HFD/CE induction led to morphological or histological alterations, conforming to the criteria for IBS animal models [11], showing the success of the IBS model. These apparent symptoms were significantly alleviated by Liupao tea. Firstly, HFD/CE rats exhibited slower growth in body length and weight loss, less desire for exploration, lethargy, and even passed out loose stools. What interested us the most was that rats with IBS acted abnormally compared to healthy rats during the open-field test. It is speculated that dysfunction of gut microbiota contributes to anxiety-like or depression-like behaviors for the link between gut microbiota and stress-related behaviors have already been discussed through the open-field test [30,31]. IBS is involved in the dysregulation of the brain-gut axis. When rats with IBS are experiencing abnormal pain or discomfort in the gastrointestinal tract, they are more likely to experience psychiatric disorders, including panic disorders, anxiety disorders, social phobia, and major depression [32]. Secondly, motilin and gastrin in serum are important hormones secreted by Mo cells and G cells, respectively, to be involved in the regulation of gastrointestinal tract function. Motilin can stimulate the contraction of gastric smooth muscle and promote gastric emptying while gastrin can accelerate gastric acid secretion and nourish the gastrointestinal mucosa [33]. D-lactic acid levels can be detected to evaluate the degree of intestinal mucosal injury and intestinal permeability [34]. Higher D-lactic acid levels were found in the M group. Last but not the least, after high-fat diet with cold exposure, infiltration occurred among epithelial mucosal cells. The maintenance of the integrity of the mucosal frontier as a barrier is indispensable for the proper functioning of the mucosa in activities such as nutrient and fluid absorption and secretion [35]. In the current study, Liupao tea showed protective effects on both gastrointestinal and renal epithelial cells. Liupao tea has been reported to modulate gastrointestinal function by promoting the colonization of beneficial bacterial strains; however, few studies have suggested that renal damage can be repaired by Liupao tea. The potential mechanism will be explained precisely as follows.

We also evaluated the effects of Liupao tea on lipid and water metabolism. Our long-term study showed that rats with IBS exhibited signs of lipid metabolism disorders, including increased TC, LDL, and TG levels. Hyperlipidemia has been considered to be part of the 'lipid turbidity' category in traditional Chinese medicine, and its causes are closely related to the spleen and stomach. High-fat and high-sucrose diets may induce splenic transport dysfunction, which leads to abnormalities in the generation, transportation, and excretion of the spleen. Functional disorders of the spleen and the stomach are involved in the pathogenesis of IBS. In addition to the TCM theory, this study demonstrates that damage to the intestinal mucosal barrier results in changes in lipid metabolism [36]. Alanine aminotransferase mainly exists in liver cells, and its content is positively correlated with hepatitis and toxic hepatitis [37]. We found that the liver coefficients and ALT levels in the model group were abnormally increased, indicating abnormal liver function. Surprisingly, the abovementioned co-morbid symptoms could be alleviated by treatment with Liupao tea.

On the grounds of the TCM theory, the kidney governs water metabolism. This indicates that the kidney regulates water metabolism. The water content, together with kidney-related indexes, was detected. Interestingly, it follows the same rule as our previous research results, showing that uric acid levels of the model group were significantly higher than those of the normal group, which implies that high uric acid can aggravate the inflammatory response by promoting the release of inflammatory factors. It has been found that uric acid crystals trigger the release of pro-inflammatory cytokines [38]. Apart from the relation with cytokines, elevated uric acid levels can also be used to predict the development of renal function deficiency in people under normal renal conditions [39]. AQP3 is considered to exert a beneficial effect in regulating the fecal water content in the colon and reabsorption work of colonic epithelial cells. Because the osmotic pressure is lower in the lumen of the colon than that on the vascular side, water molecules pass from the intestinal tract to the vascular side of the cells through AQP3, which further concentrates feces. When there is a decrease in the expression levels of AQP3, the transit of water reduces, resulting in water retention in the intestine and, thus, diarrhea [40]. In this study, HFD/CE led to an increase in the fecal water content and a decrease in the expression level of AQP3 in colon tissues; however, both indexes are reversed by Liupao tea administration. Therefore, it is speculated that Liupao tea may accelerate water transportation into the intestinal tract via the upregulation of AQP3 and the downregulation of water retention in the colon, which will reduce the fecal water content and alleviate diarrhea. Our study revealed that the expression level of AQP3 in the colonic tissue of the model group was significantly less than that of the normal group, which was consistent with the findings of a previous study on rats with IBS [12]. In

the kidney, AQP3 is mainly involved in water reabsorption and urine concentration because studies have found that the water consumption and urine volume of AQP3 knockout mice are more than 12 times higher than those of wild mice, which indicates that the urine-concentrating ability of the mice is seriously impaired [41]. According to the abnormal AQP3 expression, we suspect that aquaporin 3 may be involved in the pathogenesis of IBS. Liupao tea may contribute to the balance of water and fluid metabolism by regulating the expression of aquaporin in the gastrointestinal tract and kidneys.

According to our results, HFD/CE induction promotes the expression of pro-inflammatory cytokines. Liupao tea exerts a beneficial effect in relieving inflammation caused by HFD/CE. Lard oil-derived diet increased systemic TLR activation, triggered by a heterodimer composed of RelA and p50 in the NF-κB family [42], and white adipose tissue inflammation as well as altered microbial pattern. From what has been mentioned above, high uric acid levels can contribute to the production of pro-inflammatory cytokines. We also point out that Liupao tea exerts anti-inflammatory effects through the inhibition of pro-inflammatory cytokines, and the activation of NF-κB, TNF-α, IL-6, and IL-1β are the key pro-inflammatory cytokines identified in our study. TNF-α has been shown to play a central role in the pathogenesis of IBD by activating the NF-κB signaling pathway. The activation of NF-κB is related to the synthesis of IL-6·and IL-1β [43,44]. HFD/CE-induced rats showed a tendency to have reduced levels of TNF-α, IL-6, and IL-1β after Liupao tea treatment, which is in line with the reported results [20]. Therefore, the revealed anti-inflammatory effect of Liupao tea may be associated with the inhibition of the NF-κB pathway.

It has been known that the intestinal flora is closely related to gastrointestinal diseases. We investigated the composition and structure of the microbial community of the model rats through multiple techniques such as the α-diversity analysis, β-diversity analysis, and function prediction analysis. It was found that the gut microbiota of HFD/CE-induced rats was significantly different from that of rats in the N group. Liupao tea reversed the changes in gut microbiota diversity caused by an unhealthy lifestyle. Consistently, Liupao tea improves gut microbiota in rats challenged with HFD [17].

Our understanding of the gut microbiota of rats with IBS can be further enhanced by the remarkable changes in abundance and diversity of microbiota between the N and M groups. *Firmicutes* and *Bacteroidetes*, the two most important bacterial phyla in the gastrointestinal tract representing 90% of the gut microbiota, have gained much attention in the last decades [45]. Fecal microbiota for patients with IBS included increased *Firmicutes* and decreased *Bacteroidetes* [46]. We observed consistent changes in the *Firmicutes/Bacteroidetes* ratio. Although *Actinobacteria* and *Patescibacteria* did not show a significant difference at the phylum level, they have been reported for their nonnegligible role in IBS. *Actinobacteria* are involved in the biodegradation and biotransformation of substances introduced into the diet and gastrointestinal tract [47]. Enrichment of *Actinobacteria* was observed significantly in the patients with IBS [48]. *Actinobacteria* and *Firmicutes* dominate the fecal-associated microbiota in IBS patients [49]. *Patescibacteria* increased in the model group compared to the blank group. The long-term drug treatment sharply reduced *Firmicutes* and *Patescibacteria* [50]. There are five genus species stressed out in our study. Patients with IBS showed significantly higher counts of *Lactobacillus* than controls ($p = 0.031$). The rise in *Lactobacillus* counts results in increase in the levels of acetic acid and propionic acid in patients with IBS [51]. Species abundance of *Muribaculaceae* reduced greatly in IBS with diarrhea. *Muribaculaceae* also is reported to decrease in colitis mice [52]. Futhermore, *Ruminococcaceae* and *Lachnospiraceae* are found to decrease significantly in IBS mice [53,54]. Researchers propose that a greater abundance of *Prevotellaceae* is a feature of healthy individuals [55].

Correlation analysis was adopted to describe the correlation between biological parameters and gut microbiota. HFD/CE induction increased the *Firmicutes/Bacteroides* ratio but decreased the body weights of rats with IBS. To date, numerous studies have demonstrated that the relative abundance and relative abundance ratios of *Firmicutes* and *Bacteroides* are positively correlated with obesity. The higher the ratio, the more obese the host is [56]. This perspective contradicts our results to some extent since body weight gain did not occur in HFD/CE-induced rats. However, scientists have proved that reduced temperatures promote weight loss in obese rats [57,58]. Sustained and intermittent cold exposure may explain the body weight loss in the model group. COG function prediction illustrates there is a strong connection between alterations in lipid transport and metabolism and IBS animal model. Lipid metabolism includes the biosynthesis and degradation of lipids, such as fatty acids, TC and TG. TC, TG, HDL, and LDL are important indexes when evaluating lipid metabolism. The elevated TC, TG and LDL levels explicitly indicate Liupao tea might manage lipid transport and metabolism directly or indirectly through the regulation of gut microbiota. Intestinal bacteria produce bile acids and short chain fatty acids (SCFAs), thus indirectly modulating lipid metabolism. Bacteria produce one class of metabolites, SCFAs. Subsequently, SCFAs are metabolized by the host or act as hormones. A greater concentration of butyrate was caused by the increase of *Firmicutes/Bacteroidetes* ratio [59]. Liupao tea significantly downregulate the *Firmicutes/Bacteroidetes* ratio but upregulate the abundance of the other phylum bacteria. The remarkable decrease in the abundance of *Lactobacillus* bacterial strains should also be attached some importance in Liupao tea groups. *Lactobacillus* probiotics contributes to balancing the microbial ecology in obese animals [60] while an excessive number of *Lactobacillus* might disrupt metabolic homeostasis, increasing lipids. A positive correlation was observed between *Muribaculaceae* and butyrate production ($p < 0.05$). *Ruminococcaceae* was strongly negatively correlated with isovalerate ($p < 0.05$) [61]. Acetic and propionic acids were positively correlated with *Prevotellaceae* ($p < 0.05$) [62]. Butyrate concentrations were positively correlated with *Lachnospiraceae* ($p = 0.002$) [63]. HFD/CE-induced rats with IBS may benefit from Liupao tea administration by regulating the abundance of bacterial phyla and genera in the gut flora.

5. Conclusion

Liupao tea have various kinds of active ingredients, such as catechins, polyphenols, amino acids, caffeine, polysaccharides and other components. Liupao tea effectively improves gastrointestinal dysfunction, inflammation, and abnormal water metabolism in rats with IBS. In addition, the intervention of Liupao tea could reverse gut microbiota imbalance. The traditional Chinese medicine of Huoxiang Zhengqi oral liquid shows similar therapeutic effects to that of Liupao tea in treating IBS. This study not only fills the

knowledge gap of modern pharmacological research about the action of Liupao tea against IBS, but also provides a new idea for the daily treatment for IBS. However, our study had several limitations that should be further discussed. A more comprehensive evaluation of the IBS model is needed. Though the protective effects of Liupao tea mainly focused on rats with IBS, its preventative or therapeutic properties in people with IBS need to be further investigated. Physiological indicators should also be evaluated, and multidimensional perspectives will help clarify the underlying mechanism of Liupao tea's action. Nonetheless, this study fills the knowledge gap on the action of Liupao tea against IBS in spite of its limitations.

Author contribution statement

Danshui Zhou, Xiaotong Liu: Conceived and designed the experiments; Performed the experiments; Analyzed and interpreted the data; Contributed reagents, materials, analysis tools or data; Wrote the paper.

Lunli Lan, Wenxin Yu: Analyzed and interpreted the data; Wrote the paper.

Ruijin Qiu, Cuiqin Teng, Liyun Huang, Cuiping Yu: Contributed reagents, materials, analysis tools or data; Wrote the paper.

Yu Zeng: Analyzed and interpreted the data; Contributed reagents, materials, analysis tools or data; Wrote the paper.

Data availability statement

Data will be made available on request.

Funding statement

This work was supported by the Guangxi Innovation Driven Development Special Fund Project of China (Guike AA20302018-17) and the State Key Laboratory for Damp Syndrome of Traditional Chinese Medicine Established Jointly by the Province and the Ministry (SZ2022KF04).

Additional information

No additional information is available for this paper.

Declaration of competing interest

The authors declare that they have no known competing financial interests or personal relationships that could have appeared to influence the work reported in this paper.

Appendix A. Supplementary data

Supplementary data to this article can be found online at https://doi.org/10.1016/j.heliyon.2023.e16613.

References

[1] H.T. Xiao, L. Zhong, S.W. Tsang, Z.S. Lin, Z.X. Bian, Traditional Chinese medicine formulas for irritable bowel syndrome: from ancient wisdoms to scientific understandings, Am. J. Chin. Med. 43 (1) (2015) 1–23, https://doi.org/10.1142/S0192415X15500019.

[2] R. Teschke, A. Wolff, C. Frenzel, A. Eickhoff, J. Schulze, Herbal traditional Chinese medicine and its evidence base in gastrointestinal disorders, World J. Gastroenterol. 21 (15) (2015) 446–4490, https://doi.org/10.3748/wjg.v21.i15.4466.

[3] B.E. Lacy, F. Mearin, L. Chang, W.D. Chey, A.J. Lembo, M. Simren, R. Spiller, Bowel disorders, Gastroenterol. 150 (6) (2016) 1393–1407, https://doi.org/10.1053/j.gastro.2016.02.031.

[4] Y. Funakami, E. Itoh, T. Hata, T. Wada, S. Ichida, Specific alternation of rhythm in temperature (SART) stress-induced irritable bowel syndrome-like changes in mice and effects of drugs, Biol. Pharm. Bull. 33 (9) (2010) 1545–1549, https://doi.org/10.1248/bpb.33.1545.

[5] R.P. MacDermott, Treatment of irritable bowel syndrome in outpatients with inflammatory bowel disease using a food and beverage intolerance, food and beverage avoidance diet, Inflamm. Bowel Dis. 13 (1) (2007) 91–96, https://doi.org/10.1002/ibd.20048.

[6] A.J. Chicco, G.C. Sparagna, S.A. Mccune, C.A. Johnson, R.L. Moore, Linoleate-rich high-fat diet decreases mortality in hypertensive heart failure rats compared with lard and low-fat diets, Hypertension (Dallas) 52 (3) (2008) 549–555, https://doi.org/10.1161/HYPERTENSIONAHA.108.114264.

[7] X.K. Wang, M.J. Cheng, M. Zhao, A.G. Ge, F.F. Guo, M. Zhang, Y.H. Yang, L.G. Liu, N.H. Yang, Differential effects of high-fat-diet rich in lard oil or soybean oil on osteopontin expression and inflammation of adipose tissue in diet-induced obese rats, Eur. J. Nutr. 52 (2013) 1181–1189, https://doi.org/10.1007/s00394-012-0428-z.

[8] S. Janssens, M.M. Heemskerk, S.A. van den Berg, N.A. van Riel, K. Nicolay, K. Wilems van Dijk, P.J. prompers, Effects of low-stearate palm oil and high-stearate lard high-fat diets on rat liver lipid metabolism and glucose tolerance, Nutr. Metabol. 12 (2015) 1–11, https://doi.org/10.1186/s12986-015-0053-y.

[9] J. Yde, S.J. Keely, H.B. Moeller, Expression, regulation and function of Aquaporin-3 in colonic epithelial cells, Biochim. Biophys. Acta Biomembr. 1863 (2021), 183619, https://doi.org/10.1016/j.bbamem.2021.183619.

[10] S. Nielsen, J. Frkiaer, D. Marples, T.H. Kwon, M.A. Knepper, Aquaporins in the kidney: from molecules to medicine, Phys. Rev. 82 (1) (2002) 205–244, https://doi.org/10.1152/physrev.00024.2001.

[11] K.B. Hong, H. Seo, J.S. Lee, Y. Park, Effects of probiotic supplementation on post-infectious irritable bowel syndrome in rodent model, BMC Compl. Alternative Med. 19 (2019) 1–8, https://doi.org/10.1186/s12906-019-2610-9.

[12] G.Q. Chao, S. Zhang, Aquaporins 1, 3 and 8 expression in irritable bowel syndrome rats' colon via NF-κB pathway, Oncotarget 8 (29) (2017) 47175–47183, https://doi.org/10.18632/oncotarget.17565.

[13] S.M. Collins, A role for the gut microbiota in IBS, Nat. Rev. Gastroenterol. Hepatol. 11 (2014) 497–505, https://doi.org/10.1038/nrgastro.2014.40.

[14] X. Guo, M. Xuan, H. Zheng, S. Qin, H. Wu, S. Huang, Z. Wen, The Chinese herbal formula Huoxiang Zhengqi for diarrhea-predominant irritable bowel syndrome (CHAIRS): a study protocol for a double-blinded randomized controlled trial, Trials 22 (2021) 1–8, https://doi.org/10.1186/s13063-021-05444-w.

[15] M. Chen, J. Zhao, S. Fu, J. Yu, X. Zhang, Q. Zhang, Z. Zhou, Clinical practice of Chinese medicine navel therapy for chronic diarrhea: a literature review, J. Gastroenterol. Hepatol. 34 (4) (2019) 643–649, https://doi.org/10.1111/jgh.14549.

[16] F.J. Lin, X.L. Wei, H.Y. Liu, H. Li, R.Y. Gan, State-of-the-art review of dark tea: from chemistry to health benefits, Trends Food Sci. Technol. 109 (2021) 126–138, https://doi.org/10.1016/j.tifs.2021.01.030.

[17] Z.P. Gong, J. Ouyang, X.L. Wu, F. Zhou, M.Z. Zhu, Dark tea extracts: chemical constituents and modulatory effect on gastrointestinal function, Biomed. Pharmacother. 130 (2020), 110514, https://doi.org/10.1016/j.biopha.2020.110514.

[18] W. Ni, X. Chen, S. Wei, L. Lan, R. Qiu, Y. Ling, D. Zhou, Z. Wu, Z. Cao, C. Yu, Y. Zeng, Study on the mechanism of active components of Liupao tea on 3CL pro based on HPLC & AD fingerprint and molecular docking technique, J. Food Biochem. 45 (2021), e13707, https://doi.org/10.1111/jfbc.13707.

[19] Q. Ding, B. Zhang, W. Zheng, X. Chen, B. Ma, Liupao tea extract alleviates diabetes mellitus and modulates gut microbiota in rats induced by streptozotocin and high-fat, high-sugar diet, Biomed. Pharmacother. 118 (2019), 109262, https://doi.org/10.1016/j.biopha.2019.109262.

[20] Y. Wu, H. Sun, R. Yi, F. Tan, X. Zhao, Anti-obesity effect of Liupao tea extract by modulating lipid metabolism and oxidative stress in high-fat-diet-induced obese mice, J. Food Sci. 86 (1) (2021) 215–227, https://doi.org/10.1111/1750-3841.15551.

[21] H.Y. Joo, M.H. Nam, Y.J. Hoon, N. Chung, Y.K. Lee, UPLC-QTOF-MS/MS screening and identification of bioactive compounds in fresh, aged, and browned Magnolia denudata flower extracts, Food Res. Int. 133 (2020), 109192, https://doi.org/10.1016/j.foodres.2020.109192.

[22] W.W. Zhang, Y. Li, X.Q. Wang, F. Tian, H. Cao, M.W. Wang, Q.S. Sun, Effects of magnolol and honokiol derived from traditional Chinese herbal remedies on gastrointestinal movement, World J. Gastroenterol. 11 (28) (2005) 4414–4418, https://doi.org/10.3748/wjg.v11.i28.4414.

[23] K. Ochiai, R. Hirooka, M. Sakaino, S. Takeuchi, T. Hira, 2-Arachidonoyl glycerol suppresses gastric emptying via the cannabinoid receptor 1-cholecystokinin signaling pathway in mice, Lipids 57 (2022) 173–181, https://doi.org/10.1002/lipd.12341.

[24] Y. Yue, Z. He, Y. Zhou, R.P. Ross, C. Stanton, J. Zhao, H. Zhang, B. Yang, W. Chen, Lactobacillus plantarum relieves diarrhea caused by enterotoxin-producing Escherichia coli through inflammation modulation and gut microbiota regulation, Food Funct. 11 (2020) 10362–10374, https://doi.org/10.1039/d0fo02670k.

[25] B. Feng, P.R. Brumovsky, G.F. Gebhart, Differential roles of stretch-sensitive pelvic nerve afferents innervating mouse distal colon and rectum, Am. J. Physiol. 298 (3) (2010) 402–409, https://doi.org/10.1152/ajpgi.00487.2009.

[26] G. Cai, A. Wusiman, P. Gu, N. Mao, S. Xu, T. Zhu, J. He, Z. Liu, D. Wang, Supplementation of Alhagi honey polysaccharides contributes to the improvement of the intestinal immunity regulating the structure of intestinal flora in mice, Food Funct. 12 (2021) 9693–9707, https://doi.org/10.1039/d1fo01860d.

[27] Y. Liu, F. Yin, L. Huang, H. Teng, T. Shen, H. Qin, Long-term and continuous administration of Bacillus subtilis during remission effectively maintains the remission of inflammatory bowel disease by protecting intestinal integrity, regulating epithelial proliferation, and reshaping microbial structure and function, Food Funct. 12 (5) (2021) 2201–2210, https://doi.org/10.1039/d0fo02786c.

[28] C.J. Yao, Y.L. Li, M.J. Pu, L.H. Luo, P.M. Feng, Traditional Chinese medicine for irritable bowel syndrome: a protocol for meta-analysis, Méd. 99 (48) (2020), e23394, https://doi.org/10.1097/MD.0000000000023394.

[29] Z.M. Wu, W.X. Yu, W.J. Ni, C.Q. Teng, W.L. Ye, C.P. Yu, Y. Zeng, Improvement of obesity by Liupao tea is through the IRS-1/PI3K/AKT/GLUT4 signaling pathway according to network pharmacology and experimental verification, Phytomedicine 110 (2023), 154633, https://doi.org/10.1016/j.phymed.2022.154633.

[30] R.D. Heijtz, S. Wang, F. Anuar, Y. Qian, B. Bjorkholm, A. Samuelsson, M.L. Hibberd, H. Forssberg, S. Pettersson, Normal gut microbiota modulates brain development and behavior, Proc. Natl. Acad. Sci. USA 108 (7) (2011) 3047–3052, https://doi.org/10.1073/pnas.1010529108.

[31] R.A. Luna, J.A. Foster, Gut brain axis: diet microbiota interactions and implications for modulation of anxiety and depression, Curr. Opin. Biotechnol. 32 (2015) 35–41, https://doi.org/10.1007/s10753-011-9423-4.

[32] K. Sarah, Cognitive-behavioral therapy for patients with irritable bowel syndrome: current insights, Psychol. Res. Behav. Manag. 10 (2017) 231–237, https://doi.org/10.2147/PRBM.S120817.

[33] X.D. An, L.Y. Duan, Y.H. Zhang, D. Jin, S.H. Zhao, R.R. Zhou, Y.Y. Duan, F.M. Lian, X.L. Tong, The three syndromes and six Chinese patent medicine study during the recovery phase of COVID-19, Chin. Med. 16 (2015) 44, https://doi.org/10.1186/s13020-021-00454-x.

[34] M.J. Murray, J.J. Barbose, C.F. Cobb, Serum D(-)-lactate levels as a predictor of acute intestinal ischemia in a rat model, J. Surg. Res. 54 (5) (1993) 507–509, https://doi.org/10.1006/jsre.1993.1078.

[35] R.J. Xavier, D.K. Podolsky, Unravelling the pathogenesis of inflammatory bowel disease, Nature 448 (7152) (2007) 427–434, https://doi.org/10.1038/nature06005.

[36] K. Gallagher, A. Catesson, J.L. Griffin, E. Holmes, H. Williams, Metabolomic analysis in inflammatory bowel disease: a systematic review, J. Crohn's Colitis 15 (5) (2020) 813–826, https://doi.org/10.1093/ecco-jcc/jjaa227.

[37] S. Park, N.K. Choi, Hepatitis virus infection and age- related cataract open, Sci. Rep. 7 (1) (2017), 13089, https://doi.org/10.1038/s41598-017-13283-6.

[38] Y. Yang, H. Wang, M. Kouadir, H. Song, F. Shi, Recent advances in the mechanisms of NLRP3 inflammasome activation and its inhibitors, Cell Death Dis. 10 (2) (2019) 128, https://doi.org/10.1038/s41419-019-1413-8.

[39] R.J. Johnson, D.H. Kang, D. Feig, S. Kivlighn, J. Kanellis, S. Watanabe, K.R. Tuttle, B. Rodriguez-Iturbe, J. Herrera-Acosta, M. Mazzali, Is there a pathogenetic role for uric acid in hypertension and cardiovascular and renal disease, Hypertension (Dallas) 41 (6) (2003) 1183–1190, https://doi.org/10.1161/01.HYP.0000069700.62727.C5.

[40] R. Kon, N. Ikarashi, C. Nagoya, T. Takayama, Y. Kusunoki, M. Ishii, H. Ueda, W. Ochiai, Y. Machida, K. Sugita, Rheinanthrone, a metabolite of sennoside A, triggers macrophage activation to decrease aquaporin-3 expression in the colon, causing the laxative effect of rhubarb extract, J. Ethnopharmacol. 152 (1) (2014) 190–200, https://doi.org/10.1016/j.jep.2013.12.055.

[41] B. Yang, T. Ma, A.S. Verkman, Erythrocyte water permeability and renal function in double knockout mice lacking aquaporin-1 and aquaporin-3, J. Biol. Chem. 276 (1) (2001) 624, https://doi.org/10.1074/jbc.M008664200.

[42] T. Kawai, S. Akira, Signaling to NF-κB by toll-like receptors, Trends Mol. Med. 13 (11) (2007) 460–469, https://doi.org/10.1016/j.molmed.2007.09.002.

[43] H. Ling, Y. Tang, Q. Jiao, P. Yu, Q. Yuan, F. Zhang, L. Tao, Vasoactive intestinal peptide enhances TNF-α-induced IL-6 and IL-8 synthesis in human proximal renal tubular epithelial cells by NF-κB-dependent mechanism, Inflammation 35 (3) (2012) 1154–1160, https://doi.org/10.1007/s10753-011-9423-4.

[44] Y.K. Jung, Y.M. Kang, S. Han, Osteoclasts in the inflammatory arthritis: implications for pathologic osteolysis, Immun. Netw. 19 (1) (2019) e2, https://doi.org/10.4110/in.2019.19.e2.

[45] S. Stojanov, A. Berlec, B. Štrukelj, The influence of probiotics on the firmicutes/bacteroidetes ratio in the treatment of obesity and inflammatory bowel disease, Microorgansims 8 (11) (2020) 1715.

[46] R. Duan, S. Zhu, B. Wang, L. Duan, Alterations of gut microbiota in patients with irritable bowel syndrome based on 16S rRNA-targeted sequencing: a systematic review, Clin. Transl. Gastroenterol. 10 (2) (2019), e00012, https://doi.org/10.14309/ctg.0000000000000012.

[47] C. Binda, L.R. Lopetuso, G. Rizzatti, G. Gibiino, V. Cennamo, A. Gasbarrini, Actinobacteria: a relevant minority for the maintenance of gut homeostasis, Dig. Liver Dis.: Off. J. Ital. Soc. Gastroenter. Ital. Assoc. Study Liv. 50 (5) (2018) 421–428, https://doi.org/10.1016/j.dld.2018.02.012.

[48] I. Masoodi, A.S. Alshanqeeti, E.J. Alyamani, A.A. Allehibi, A.N. Alqutub, K.N. Alsayari, A.O. Alomair, Microbial dysbiosis in irritable bowel syndrome: a single-center metagenomic study in Saudi Arabia, JGH Open 4 (4) (2020) 649–655, https://doi.org/10.1002/jgh3.12313.

[49] I. Rangel, J. Sundin, S. Fuentes, D. Repsilber, W.M.D. Vos, R.J. Brummer, The relationship between faecal-associated and mucosal-associated microbiota in irritable bowel syndrome patients and healthy subjects, Aliment. Pharm. Therap. 42 (2015) 1211–1221, https://doi.org/10.1111/apt.13399.

[50] Y. Wang, Y. Zou, J. Wang, H. Ma, B. Zhang, S. Wang, The protective effects of 2'-fucosyllactose against E. Coli O157 infection are mediated by the regulation of gut microbiota and the inhibition of pathogen adhesion, Nutrients 12 (5) (2020) 1284, https://doi.org/10.3390/nu12051284.

[51] C. Tana, Y. Umesaki, A. Imaoka, T. Handa, S. Fukudo, Altered profiles of intestinal microbiota and organic acids may be the origin of symptoms in irritable bowel syndrome, Neuro Gastroenterol. Motil. 22 (4) (2010) 512-e115, https://doi.org/10.1111/j.1365-2982.2009.01427.x.
[52] S. Guo, W. Geng, S. Chen, L. Wang, Y. Lu, Ginger alleviates DSS-induced ulcerative colitis severity by improving the diversity and function of gut microbiota, Front. Pharmacol. 12 (2021), 632569, https://doi.org/10.3389/fphar.2021.632569.
[53] T. Su, R. Liu, L. Allen, Y. Long, L. Du, S. Lai, X. Chen, L. Wang, J. Si, O. Chung, Altered intestinal microbiota with increased abundance of prevotella is associated with high risk of diarrhea-predominant irritable bowel syndrome, Gastroenterol. Res. Pract. 2018 (2018) 1–9, https://doi.org/10.1155/2018/6961783.
[54] Q.S. Wang, Y.L. Wang, W.Y. Zhang, K.D. Li, X.F. Luo, Y.L. Ci, Puerarin from Pueraria lobata alleviates the symptoms of irritable bowel syndrome-diarrhea, Food Funct. 12 (2021) 2211–2224, https://doi.org/10.1039/d0fo02848g.
[55] D.B. Gootenberg, J.M. Paer, J.M. Luevano, D.S. Kwon, HIV-associated changes in the enteric microbial community: potential role in loss of homeostasis and development of systemic inflammation, Curr. Opin. Infect. Dis. 30 (1) (2017) 31–34, https://doi.org/10.1097/QCO.0000000000000341.
[56] R.E. Ley, P.J. Turnbaugh, S. Klein, J.I. Gordon, Microbial ecology - human gut microbes associated with obesity, Nature 444 (2006) 1022–1023, https://doi.org/10.1038/4441022a.
[57] Y. Meng, L. Chen, W. Lin, H. Wang, X. Weng, Exercise reverses the alterations in gut microbiota upon cold exposure and promotes cold-induced weight loss, Front. Physiol. 11 (2020) 311, https://doi.org/10.3389/fphys.2020.00311.
[58] M. Zietak, P. Kovatcheva-Datchary, L. Markiewicz, M. Ståhlman, L. Kozak, F. Bäckhed, Altered microbiota contributes to reduced diet-induced obesity upon cold exposure, Cell Metabol. 23 (6) (2016) 1216–1223, https://doi.org/10.1016/j.cmet.2016.05.001.
[59] S. Louis-Jean, D. Martirosyan, Nutritionally attenuating the human gut microbiome to prevent and manage metabolic syndrome, J. Agric. Food Chem. 67 (46) (2019) 12675–12684, https://doi.org/10.1021/acs.jafc.9b04879.
[60] F. Yan, N. Li, J. Shi, H. Li, B. Li, Lactobacillus acidophilus alleviates type 2 diabetes by regulating hepatic glucose, lipid metabolism and gut microbiota in mice, Food Funct. 10 (9) (2019) 5804–5818, https://doi.org/10.1039/c9fo01062a.
[61] Y. Li, D. Xia, J. Chen, X. Zhang, H. Wang, L. Huang, J. Shen, S. Wang, Y. Feng, D. He, Dietary fibers with different viscosity regulate lipid metabolism via ampk pathway: roles of gut microbiota and short-chain fatty acid, Poultry Sci. 101 (4) (2022), 101742, https://doi.org/10.1016/j.psj.2022.101742.
[62] Y. Wang, L. Li, C. Ye, J. Yuan, S. Qin, Alginate oligosaccharide improves lipid metabolism and inflammation by modulating gut microbiota in high-fat diet fed mice, Appl. Microbiol. Biotechnol. 104 (11) (2020) 3541–3554, https://doi.org/10.1007/s00253-020-10449-7.
[63] S.I. Choi, J.H. Son, N. Kim, Y.S. Kim, Y.J. Seok, Changes in cecal microbiota and short-chain fatty acid during lifespan of the rat, J. Neurogastr. Motil. 27 (1) (2021) 134–146, https://doi.org/10.5056/jnm20148.